AJRCCM Articles in Press. Published on 21-November-2017 as 10.1164/rccm.201707-1475OC

B cells producing type I interferon modulate macrophage polarization in tuberculosis

Alan Bénard[1,2,3], Imme Sakwa[4], Pablo Schierloh[2,5], André Colom[1,2], Ingrid Mercier[1,2,6], Ludovic Tailleux[7,8], Luc Jouneau[9], Pierre Boudinot[9], Talal Al-Saati[10], Roland Lang[11], Jan Rehwinkel[12], Andre G. Loxton[13], Stefan H. E. Kaufmann[14], Véronique Anton-Leberre[6], Anne O'Garra[15,16], Maria Del Carmen Sasiain[2,5], Brigitte Gicquel[9], Simon Fillatreau[4,17,18,19#], Olivier Neyrolles[1,2#], Denis Hudrisier[1,2,20#]

[1]Institut de Pharmacologie et de Biologie Structurale, Université de Toulouse, CNRS, UPS, France
[2]International associated laboratory (LIA) CNRS "IM-TB/HIV" (1167), Toulouse, France, and Buenos Aires, Argentina
[3]Translational Research Center, Universitätsklinikum Erlangen, Department of Surgery, Erlangen, Germany
[4]Deutsches Rheuma-Forschungszentrum, a Leibniz Institute, Charitéplatz 1, 10117 Berlin, Germany
[5]IMEX-CONICET, Academia Nacional de Medicina, Pacheco de Melo 3081, 1425 CABA, Argentina
[6]LISBP, Université de Toulouse, CNRS, INRA, INSA, Toulouse, France
[7]Institut Pasteur, Unit of Mycobacterial Genetics, 75015 Paris, France
[8] Institut Pasteur, Unit for Integrated Mycobacterial Pathogenomics, 75015 Paris, France
[9]Virologie et Immunologie Moléculaires, INRA, 78352 Jouy-en-Josas, France
[10]INSERM/UPS/ENVT - US006/CREFRE, Service d'Histopathologie, CHU Purpan, Toulouse, France.
[11]Institute of Clinical Microbiology, Immunology and Hygiene, University Hospital Erlangen, Friedrich-Alexander-University Erlangen-Nürnberg Erlangen, Germany
[12]Medical Research Council Human Immunology Unit, Medical Research Council Weatherall Institute of Molecular Medicine, Radcliffe Department of Medicine, University of Oxford, Oxford OX3 9DS, UK
[13]SA MRC Centre for TB Research, DST/NRF Centre of Excellence for Biomedical Tuberculosis Research, Division of Molecular Biology and Human Genetics, Faculty of Medicine and Health Sciences, Stellenbosch University, PO Box 241 Cape Town, 8000 South Africa
[14]Max Planck Institute of Infection Biology, Department of Immunology, Charitéplatz 1, 10117 Berlin, Germany
[15]Division of Immunoregulation, MRC National Institute for Medical Research, London, UK
[16]NHLI, Faculty of Medicine, Imperial College London, London, UK
[17]Institut Necker-Enfants Malades (INEM), INSERM U1151-CNRS UMR 8253, Paris, France
[18]Université Paris Descartes, Sorbonne Paris Cité, Faculté de Médecine, Paris, France
[19]Assistance Publique - Hôpitaux de Paris (AP-HP), Hôpital Necker Enfants Malades, Paris, France
[20]Correspondence should be addressed to D.H., Institut de Pharmacologie et de Biologie Structurale, CNRS & Université de Toulouse, Université Paul Sabatier, 205 route de Narbonne, 31000 Toulouse, France, Tel: + 33 (0) 5 61 17 59 10, Fax: + 33 (0) 5 61 17 59 90, Email: denis.hudrisier@ipbs.fr
[#]These authors contributed equally to the work.

Author contribution. A.B. performed most of the experiments and data analysis, designed the study and wrote the manuscript. I.S., P.S., A.C., L.T. B.G and T.A.S. contributed to some experiments. I.M., L.J., P.B. and V.A.L. performed the microarray data analysis. P.S., R.L., J.R. M.D.C.S. A.L. and A.O.G. provided key biological material. S.H.E.K. helped with the writing of the manuscript. S.F., O.N. and D.H. designed the study, performed some experiments, and wrote the manuscript.

Sources of support. This work was supported by CNRS, University of Toulouse - Université Paul Sabatier, Institut Pasteur, Agence Nationale de la Recherche (Grants B-TB ANR-12-BSV3-0002 and ANR-11-EQUIPEX-0003 to O.N.), the European Union (Grants NEWTBVAC n°241745 and TBVAC2020 n°643381 to O.N. and S.H.E.K., Grant ERA-INFECT ABIR to S.F. and S.H.E.K), the Bettencourt-Schueller Foundation, the Fondation pour la Recherche Médicale (FRM, grant DEQ20160334902 to O.N.), the Deutsche Forschungsgemeinschaft (SFB 796, TP B6 to R.L., SFB TRR10 to S.F.). A.B. held a fellowship from the FRM.

Running title: B cells polarize macrophages in tuberculosis

Descriptor number: 11.4 Mycobacterial Disease: Host Defense

Word counts: 3500

This article has an online data supplement, which is accessible from this issue's table of content online at www.atsjournals.org.

AJRCCM Articles in Press. Published on 21-November-2017 as 10.1164/rccm.201707-1475OC

At a Glance Commentary.

Scientific Knowledge on the Subject

The role played by T cells in tuberculosis (TB) has been thoroughly investigated. In marked contrast the contribution of B cells in immunity to TB, which has mostly been explored for their ability to produce antibodies, remains poorly understood despite their massive accumulation in lung lesions of both TB patients and experimentally infected animals.

What This Study Adds to the Field

Here we show that B cells can be directly stimulated by *M. tuberculosis* in an innate manner to produce type I interferon (IFN) to subsequently modulate the polarization of macrophages towards a regulatory/anti-inflammatory profile *in vitro* and in infected lungs. This pathway was observed in a murine model of TB, and studying B cells isolated from TB patients. Our observations reveal B cells as novel regulators of immunity to TB through type I IFN-mediated polarization of myeloid cells.

Abstract

Rationale. In addition to their well-known function as antibody-producing cells, B lymphocytes can markedly influence the course of infectious or non-infectious diseases via antibody-independent mechanisms. In tuberculosis, B cells accumulate in lungs, yet their functional contribution to the host response remains poorly understood.

Objectives. To document the role of B cells in tuberculosis in an unbiased manner.

Methods. We generated the transcriptome of B cells isolated from *Mycobacterium tuberculosis (Mtb)*-infected mice, and validated the identified key pathways using *in vitro* and *in vivo* assays. The obtained data were substantiated using B cells from pleural effusion of tuberculosis patients.

Measurements and main results. B cells isolated from *Mtb*-infected mice displayed a STAT1-centered signature, suggesting a role for interferons in B cell response to infection. B cells stimulated *in vitro* with *Mtb* produced type I interferon, via a mechanism involving the innate sensor STING, and antagonized by MyD88 signaling. *In vivo*, B cells expressed type I interferon in the lungs of *Mtb*-infected mice and, of clinical relevance, in pleural fluid from patients with tuberculosis. Type I interferon expression by B cells induced an altered polarization of macrophages towards a regulatory/anti-inflammatory profile *in vitro*. *In vivo*, increased provision of type I interferon by B cells in a murine model of B cell-restricted *Myd88*-deficiency correlated with an enhanced accumulation of regulatory/anti-inflammatory macrophages in *Mtb* infected lungs.

Conclusion. Type I interferon produced by *Mtb*-stimulated B cells favors macrophage polarization towards a regulatory/anti-inflammatory phenotype during *Mtb* infection.

Abstract counts: 241 words

Keywords: B lymphocytes - macrophages - tuberculosis - interferon

AJRCCM Articles in Press. Published on 21-November-2017 as 10.1164/rccm.201707-1475OC

Introduction

Infection with *Mycobacterium tuberculosis* (Mtb) leads to the formation of lung lesions, the granulomas, which contain macrophages and other cell types, and are surrounded by various lymphocyte populations, including B lymphocytes (1–4). The presence of B cells at the site of infection suggests that they may contribute to host-pathogen interaction locally. Several studies attempted to delineate the antibody-mediated roles of B cells, and the impact of their total deficiency in tuberculosis (TB) (5–10). Studies performed with B cell-deficient mice yielded conflicting results, with some studies concluding that B cells played no apparent function in TB, while others concluded that B cells contributed to protection against Mtb (2, 6, 8, 11, 12). In human, the depletion of B cells in patients treated by rituximab did not increase the risk of TB reactivation (13, 14), while in macaques rituximab administration to Mtb-infected animals had limited effects at the individual granuloma level (15). These studies suggest a moderate role for B cells in immunity to Mtb. However, they used approaches that might not be suitable to reveal more complex functions of B cells, in particular those mediated through the production of cytokines, whose relevance during infection by intracellular bacterial pathogens has received increasing experimental evidence (16–18). Indeed, B cells can play either favorable or detrimental roles during infection, depending on the cytokines they produce, and the depletion of the whole B cell compartment may not be suitable to reveal such potentially antagonistic B cell activities. The aim of our study was to investigate the eventual antibody-independent functions of B cells in an unbiased manner. For this, we analyzed the transcriptome of B cells isolated from the lungs and spleen of Mtb-infected mice. This revealed a STAT1-centered signature, which pointed to the ability of B cells to both produce and respond to type I interferon (IFN). We identified STING and Mincle as positive regulators, and myeloid differentiation primary response gene 88 (MyD88) as a negative regulator of type I IFN production by Mtb-stimulated B cells. Type I IFN production

by B cells drove macrophages towards an anti-inflammatory phenotype *in vitro*. Mice with a B cell-specific *Myd88*-deficiency harbored B cells that overexpressed type I IFN, and displayed an abnormal accumulation of anti-inflammatory myeloid cells in infected lungs compared to controls. This was associated with reduced signs of inflammation and increased Mtb burden in lungs. Importantly, B cells purified from the pleural fluid of TB patients displayed a massive type I IFN expression, and supernatants of Mtb-stimulated human B cells also polarized human macrophages towards an anti-inflammatory profile *in vitro*. Altogether our data reveal that type I IFN expression in B cells impacts macrophage polarization towards an anti-inflammatory/regulatory phenotype during TB, and unravel a previously unanticipated role for B cells in this disease.

Methods

TB Patients. Human studies were performed in accordance with the Declaration of Helsinki (2013) of the World Medical Association, and have been approved by the Ethics Committees of Hospital F.J Muñiz, Academia Nacional de Medicina and Instituto Vaccarezza from Buenos Aires, Argentina. TB patients with or without moderate and large pleural effusions were identified at the Servicio de Tisioneumonología. Written informed consent was obtained before sample collection.

Mice. All mice were on the C57BL/6 background. All of the procedures including animal studies were conducted in strict accordance with French laws and regulations in compliance with the European Community council directive 68/609/EEC guidelines and its implementation in France. All protocols were approved by the Comité d'Ethique Midi-Pyrénées (MP/11/13/02/11 and MP/07/80/11/12).

Full methods are provided in online data supplements.

AJRCCM Articles in Press. Published on 21-November-2017 as 10.1164/rccm.201707-1475OC

Results

B cells purified from the lungs and spleen of Mtb-infected mice display a STAT1-centered gene expression signature. To address whether B cells might perform antibody-independent functions in TB, as observed in other bacterial infections (17–19), we performed a genome-wide transcriptome analysis of B cells isolated from the lungs and spleen of Mtb-infected mice, in comparison to splenic B cells from naive mice. Strikingly, B cells from infected mice differentially expressed a limited number (30) of genes (Figure 1A and Table E1 online) compared to naive controls. Ingenuity pathway analysis indicated that the differentially expressed genes formed a network centered on STAT1, a master transcription factor of the IFN response (Figure 1B). The higher expression of the STAT1 signature genes *Stat1*, *Irgm1*, *Csf1*, *Ccrl2*, *Ccl5* and *Cxcl9* in B cells from the lungs of infected mice was confirmed by RT-qPCR (Figure 1C and D).

Type I IFN are chief cytokines induced in lung B cells upon Mtb infection and reflect an innate B cell response. Interrogation of the Interferome database (20) indicated that 20 out of the 30 genes of the B-cell signature were regulated by both type I and type II, but not by type III IFN, and that 5 of them, namely *Mllt3*, *Hspa1a*, *Isg20*, *Gls* and *Klrd1*, were specifically regulated by type I IFN (Figure 2A), suggesting that the STAT1 signature reflected an effect of type I IFN on B cells. Consistent with this possibility, naive B cells stimulated with type I IFN *in vitro* displayed a similar gene signature (Figure 2B), and B cells recovered from the lungs of Mtb-infected mice at 3-weeks post-infection showed increased STAT1 phosphorylation after stimulation with type I IFN *ex vivo* (Figure 2C). Taken together, these data suggest that B cells were exposed to type I IFN in infected mice. Because type I IFN could act in an autocrine manner (21), we next investigated whether B cells expressed type I IFN during infection. B cells isolated from the lungs and spleen of infected mice indeed

displayed a massive up-regulation of the *Ifnb* transcripts, compared to B cells from naive mice (Figure 2D). In comparison, the levels of interleukin (*Il)-6* and *Il-10* mRNA, which have previously been identified as important mediators of the antibody-independent functions of B cells in other diseases (16, 19), showed only a modest increase (although significant in for *Il-6)* (Figure 2D). Thus, type I IFN are the chief cytokines induced in lung B cells upon Mtb infection. This possibly involved a direct interaction between Mtb and B cells because Mtb elicited type I IFN expression in naive spleen B cells *in vitro* within 24 hours (Figure 2E and F). Similar results were obtained after 4 hours of stimulation (Figure E1 online), underlining a rapid innate response. B cell-derived type I IFN protein was detected in the B cell culture supernatants using a type I IFN-specific reporter cell line (Figure 2G) and ELISA (Figure 2H). Type I IFN amplified its induction in an autocrine manner since its expression was markedly reduced in B cells lacking the type I IFN receptor subunit IFNAR1 (Figure 2I). B cells infection *per se* was not necessary as filtered supernatants from Mtb cultures also induced type I IFN expression in B cells, implicating secreted Mtb components in this process (Figure 2J). We conclude that B cells produce and respond to type I IFN during Mtb infection.

Type I IFN expression in Mtb-stimulated B cells involves innate receptors. We next sought to identify the molecular mechanisms controlling type I IFN expression in B cells exposed to Mtb, and tested the involvement of distinct innate sensors. The cytosolic dinucleotide sensor STING (22, 23) contributed to type I IFN expression in B cells stimulated with Mtb or cyclic-di-AMP (c-di-AMP), a secreted mycobacterial STING ligand (Figure 3A-D) (22, 24). In addition, the C-type lectin Mincle (25) also contributed to type I IFN expression in B cells stimulated with Mtb, albeit to a lower extent than STING (Figure E2 online). We thus used c-di-AMP to further address which B cell subset(s) contributed to this response. $CD21^{low}CD23^{hi}$ follicular and $CD21^{-}CD23^{-}$ B cells contributed most to type I IFN

AJRCCM Articles in Press. Published on 21-November-2017 as 10.1164/rccm.201707-1475OC

production (Figure 3E). This particular mode of activation could operate in lung B cells because B cells from Mtb-infected lungs also expressed type I IFN upon c-di-AMP stimulation, although in smaller amounts than non-B cells taken for comparison (Figure 3F). Testing the role of other innate receptors, we found that type I IFN expression in B cells could also be triggered by a TLR3 ligand, suggesting a role for the adaptor TIR-domain-containing adapter-inducing interferon-β (TRIF), but not by ligands of TLR7/8 or 9, which signal via MyD88 (Figure 3G and H).

Type I IFN production by B cells upon Mtb stimulation is antagonized by MyD88 signaling. We next tested the effect of MyD88 signalling on type I IFN expression in Mtb-stimulated B cells. *Myd88* deficiency resulted in an increased type I IFN expression at both transcriptional (Figure 4A) and protein (Figure 4B) levels. Accordingly, stimulation of B cells with the TLR2 agonists Pam_3CSK_4, which signals via MyD88, down-regulated type I IFN expression induced by the agonists of STING (Figure 4C) or Mincle (Figure 4D), or Mtb (Figure 4E). As expected, IL-1β also inhibited type I IFN expression in B cells in a MyD88-dependent manner (Figure 4F and G). In sum, we found that the amount of type I IFN produced by B cells is regulated by the balance between distinct innate signaling pathways. These results illustrate further the possible antagonism between TLR-MyD88 and IFN signaling (26–28).

Pleural fluid B cells express type I IFN in TB patients. An excessive type I IFN signature distinguished patients with TB from latently Mtb-infected individuals (29, 30). In order to address whether B cells could contribute to the type I FN response in TB, we next assessed whether human B cells produced and responded to type I IFN upon Mtb stimulation *in vitro*, and whether this pathway was operative in clinical TB. Human B cells purified from the

blood of healthy donors up-regulated type I IFN (both α and β) expression upon stimulation with Mtb (Figure 5A and B) or c-di-AMP (Figure 5C) *in vitro*. Remarkably, B cells from the pleural fluid (PF) of patients with TB displayed a markedly increased abundance of type I IFN transcripts, compared to B cells purified from the blood of healthy donors or patients with TB, indicating that this response was particularly present in infected lungs during disease (Figure 5D). PF B cells also responded to type I IFN *in vivo* since they displayed an increased expression of *BSTM2* and *CXCL10* (Figure 5E and F), two genes belonging to the type I IFN signature in patients with active TB (29). These results show that B cells locally express and respond to type I IFN in the infected lungs during clinical TB.

Mtb-stimulated B cells drive macrophage polarization toward an anti-inflammatory/regulatory profile in both mouse and human. Considering that B cells can directly influence the activity of cells located in their microenvironment through cytokine production (16, 19), are in close contact with macrophages in TB lesions (31), and have already been shown to modulate macrophage activity (18, 32, 33), we next assessed whether type I IFN produced by Mtb-stimulated B cells could affect macrophage polarization. Macrophages treated with the supernatant from Mtb-stimulated B cells exhibited an enhanced expression of *Cox2*, *Nos2* and *Ym1* (Figure 6A), which depended upon type I IFN (Figure 6B). A profound IFNAR1-dependent induction of IFN-stimulated genes, including *Ccl2* and *Tnfsf10* was also triggered in treated macrophages (Figure E3 online). In addition, these macrophages displayed an enhanced expression of the regulatory/anti-inflammatory molecules PD-L1 and IL-10 (Figure 6C-D and Figure E4 online), as well as a decreased production of IL-1β (Figure E4B online). A similar IFNAR-1-dependent expression profile was triggered in macrophages treated with the supernatant of c-di-AMP-stimulated B cells, confirming the involvement of type I IFN triggered by STING in this altered macrophage

AJRCCM Articles in Press. Published on 21-November-2017 as 10.1164/rccm.201707-1475OC

polarization (Figure E5 online). Similarly, supernatant of Mtb-activated human B cells induced human macrophages to express IFN-stimulated genes, such as *CCL2* (Figure 6E), and PD-L1 (Figure 6F-G). These results demonstrate that type I IFN produced by Mtb-activated B cells can directly drive macrophages towards an anti-inflammatory/regulatory phenotype, and suggest that B cells can directly influence adjacent macrophages via the local production of type I IFN in patients with active TB.

Excessive production of type I IFN by B cells is associated with altered macrophage polarization in the lungs of Mtb-infected mice. Because increased levels of type I IFN were associated with clinical TB (29), and because B cells from the PF of TB patients expressed high levels of type I IFN (Figure 5D), we investigated the consequence of type I IFN overexpression in B cells in the mouse. To generate a model in which only B cells over-express type I IFN, we took advantage of the fact that type I IFN production by B cells was inhibited by MyD88 signaling. Therefore we generated mixed BM chimera (34, 35) in which only B cells lacked MyD88 (B-*Myd88*$^{-/-}$), as well as their corresponding controls with wild-type B cells (B-WT, B-CTRL). As expected, B cells from the lungs of Mtb-infected B-*Myd88*$^{-/-}$ mice expressed more type I IFN transcripts than their controls (Figure 7A). Remarkably, B-*Myd88*$^{-/-}$ mice harbored in lungs an increased proportion of CD11b^{int}Gr1^{int} cells (Figure 7B and C), resembling a population of Mtb-permissive monocytes/macrophages known to develop in a type I IFN-dependent manner (36). Further characterization of CD11b^{int}Gr1^{int} cells from infected mice revealed that they expressed high levels of *Arg1, Cox2, iNOS* and *Ym1* compared to "classical" macrophages (Figure 7D). These data suggest that B-*Myd88*$^{-/-}$ mice display an increased accumulation of anti-inflammatory monocytes/macrophages compared to control mice. In keeping with this, they also showed in total lung an increased expression of genes characteristic of anti-inflammatory and tissue

repair-driving M2 macrophages, such as *Ym1* and *Mrc1* (37, 38) (Figure 7E), with other genes associated with M2 macrophages showing a similar trend to increased expression (*Fizz1)* or unaffected (*Arg1*) (Figure 7E), compared to controls. In contrast, the pro-inflammatory genes *Ifng*, *Tnfa*, *Nos2* and *Irgm1* were expressed at lower levels in infected chimeric animals compared to controls (Figure 7E). These data are therefore consistent with our initial hypothesis that B-*Myd88*$^{-/-}$ mice would, as a result of excessive type I IFN production by B cells, show an altered macrophage polarization towards an anti-inflammatory/regulatory profile. This B cell-mediated effect specifically affected macrophages since similar frequencies of infiltrating T (both CD4+ and CD8+) and B cells were observed in B-*Myd88*$^{-/-}$ mice compared to their B-WT counterparts (Figure E6A online). Of note, the altered macrophage phenotype in B-*Myd88*$^{-/-}$ was associated with slightly increased Mtb loads (Figure E6B online) and reduced signs of inflammation in lungs (Figure E6C online). Collectively, our data reveal that innate production of type I IFN by B cells correlates with an altered polarization of lung macrophages during Mtb infection.

Discussion

Our study reveals that innate signaling in B cells leads, through type I IFN production, to the modulation of macrophage polarization in TB. In particular, our data demonstrate that upon Mtb stimulation, B cells of murine or human origin produce type I IFN. Although B cells produce only low amounts of these cytokines, such low amounts have already been reported for type I IFN in other settings, and thus appear to be a normal feature of the type I IFN response (39). Here, we found that type I IFN production by Mtb-stimulated B cells was regulated by the integration of several pathways, whose dysregulation led to important functional consequences in TB. At the molecular level, we identified several ligands, together with their corresponding host sensors, namely STING and, to a lesser extent, Mincle, as

AJRCCM Articles in Press. Published on 21-November-2017 as 10.1164/rccm.201707-1475OC

contributors to type I IFN expression in B cells during Mtb stimulation. We also show that intrinsic MyD88 signaling, associated to either TLR or IL-1 receptor triggering, is a potent inhibitor of type I IFN production by B cells, which further illustrates the antagonism between MyD88 signaling and IFN production (28). Whether additional pathways such as the TRIF-dependent one could be involved in type I IFN production by B cells remains to be explored, yet seems likely given the capacity of TLR3 agonist to trigger such a response.

From a clinical viewpoint, we report that type I IFN expression in B cells is dramatically increased in the PF of TB patients compared to peripheral blood B cells of TB patients or healthy donors. This is in contrast with the reported type I IFN signature observed in blood myeloid cells of TB patients, compared to latently infected individuals or healthy subjects (29, 30, 40) but similar to the situation reported in blood T cells of TB patients (31). We can think of three possible explanations for the local expression of type I IFN in TB. First, it is possible that lymphocytes are in non-responsive state specifically in blood in TB. This would be consistent with the fact that peripheral B cells from TB patient have been reported to be hypo-responsive to stimulation (41). Alternatively, this might reflect a preferential trapping of modulated lymphocytes in the lungs and possibly secondary lymphoid organs, while modulated myeloid cells might be more prone to circulate from the affected tissue to the blood. Finally, this might indicate a different threshold of activation for B cells and myeloid cells by Mtb, so that B cells only respond to Mtb-derived molecules when these are present at a high concentration such as in the infected lung, but not in the blood, while myeloid cells might be able to respond to the lower microbial compound concentrations in blood**.** Thus, our data suggest that type I IFN production by B cells might be important locally, at the site of TB infection and inflammation. B cells are known to be in close proximity to other immune cells, including monocytes and macrophages, in the lungs of TB patients or infected animals (3, 31). Our *in vitro* data unambiguously demonstrate that Mtb-stimulated B cells drive

macrophage polarization towards an anti-inflammatory profile in a type I IFN-dependent manner. B cells were previously reported to modulate macrophage polarization in various models of infection, autoimmunity and cancer (18, 32, 42). In particular, B cells polarized macrophages towards an alternatively activated M2 state through IL-10 production in a murine melanoma model (42). By contrast, a similar action of B cells on macrophages was reported to be independent of IL-10 in the context of TB (33). Our data provide direct evidence that type I IFN produced by Mtb-stimulated B cells contributes to macrophage polarization *in vitro*, which might explain this apparent discrepancy. This is in agreement with our *in vivo* data showing that over-production of type I IFN by B cells in a mouse model of B cell-restricted *Myd88*-deficiency correlates with the accumulation of anti-inflammatory/regulatory macrophages during Mtb infection in infected lungs, which is locally associated with increased bacterial burden and reduced pathology.

Overexpression of type I IFN is generally detrimental in TB (43, 44). In particular hypervirulent strains of Mtb induce increased production of type I IFN (45, 46) and patients with active TB disease show a type I IFN-inducible gene expression profile in their blood cells (29, 47). Among the proposed mechanisms for the detrimental action of type I IFN in TB is the induction of IL-10 secretion by myeloid cells and macrophages, which leads to a reduced expression of protective IL-12 and TNFα (28, 43), as well as an increased induction of myeloid-derived suppressor cells (36, 48) known to be permissive for Mtb replication (48). Here we show that type I IFN over-production by B cells in our mouse model of B cell-restricted *Myd88*-deficiency is associated with an accumulation of $CD11b^{int}Gr1^{int}$ cells. Myeloid cells sharing similar phenotypic characteristics were previously reported as Mtb-permissive macrophages, whose accumulation depended on type I IFN (37). Because MyD88 signaling controls the production of IL-6 and IL-10 by B cells (49), we cannot exclude that these cytokines play a part in the observed phenotype. However, beyond the fact that the

AJRCCM Articles in Press. Published on 21-November-2017 as 10.1164/rccm.201707-1475OC

major cellular changes observed in B-*Myd88*$^{-/-}$ mice are known to be inducible by type I IFN, we do not favor this possibility because *Il6* and *Il10* mRNA were only induced at modest levels in B cells isolated from the lungs of WT mice, and it is most likely that their expression was even lower in *Myd88*-deficient B cells.

Overall, hyper-production of type I IFN production by B cells correlates with increased Mtb burden in lungs, which suggests that this B cell activity negatively affects the control of bacterial replication, and is in agreement with the thought that type I IFN are detrimental in TB. How low concentrations of type I IFN can induce significant biological responses is a complex question, whose answer likely rest on parameters such as the diversity of type I IFNs, their differential affinity for the IFNAR receptor, the properties of type I IFN signalling pathways, the timing and duration of expression (50). In conclusion, our study reveals type I IFN production as a novel antibody-independent function of B cells in immunity to TB.

Acknowledgments

We thank G. Lugo-Villarino for helpful comments. We thank F. Moreau and L. Lepourry for help with animal experiments, F. Capilla for technical assistance in histology and L. Trouilh and S. Lamarre for help with microarrays experiments and statistical analysis. We thank A. Debin for the kind gift of reagents and G. Czapliki for help with statistical analysis.

References

1. Kahnert A, Hopken UE, Stein M, Bandermann S, Lipp M, Kaufmann SH. Mycobacterium tuberculosis triggers formation of lymphoid structure in murine lungs. *J Infect Dis* 2007;195:46–54.
2. Maglione PJ, Xu J, Chan J. B cells moderate inflammatory progression and enhance bacterial containment upon pulmonary challenge with Mycobacterium tuberculosis. *J Immunol* 2007;178:7222–34.
3. Tsai MC, Chakravarty S, Zhu G, Xu J, Tanaka K, Koch C, Tufariello J, Flynn J, Chan J. Characterization of the tuberculous granuloma in murine and human lungs: cellular composition and relative tissue oxygen tension. *Cell Microbiol* 2006;8:218–32.
4. Ulrichs T, Kosmiadi GA, Trusov V, Jorg S, Pradl L, Titukhina M, Mishenko V, Gushina N, Kaufmann SH. Human tuberculous granulomas induce peripheral lymphoid follicle-like structures to orchestrate local host defence in the lung. *J Pathol* 2004;204:217–28.
5. Chan J, Mehta S, Bharrhan S, Chen Y, Achkar JM, Casadevall A, Flynn J. The role of B cells and humoral immunity in Mycobacterium tuberculosis infection. *Semin Immunol* 2014;26:588–600.
6. Kozakiewicz L, Chen Y, Xu J, Wang Y, Dunussi-Joannopoulos K, Ou Q, Flynn JL, Porcelli SA, Jacobs WR Jr, Chan J. B cells regulate neutrophilia during Mycobacterium tuberculosis infection and BCG vaccination by modulating the interleukin-17 response. *PLoS Pathog* 2013;9:e1003472.
7. Kozakiewicz L, Phuah J, Flynn J, Chan J. The role of B cells and humoral immunity in Mycobacterium tuberculosis infection. *Adv Exp Med Biol* 2013;783:225–50.
8. Johnson CM, Cooper AM, Frank AA, Bonorino CB, Wysoki LJ, Orme IM. Mycobacterium tuberculosis aerogenic rechallenge infections in B cell-deficient mice. *Tuber Lung Dis* 1997;78:257–61.
9. Lu LL, Chung AW, Rosebrock TR, Ghebremichael M, Yu WH, Grace PS, Schoen MK, Tafesse F, Martin C, Leung V, Mahan AE, Sips M, Kumar MP, Tedesco J, Robinson H, Tkachenko E, Draghi M, Freedberg KJ, Streeck H, Suscovich TJ, Lauffenburger DA, Restrepo BI, Day C, Fortune SM, Alter G. A Functional Role for Antibodies in Tuberculosis. *Cell* 2016;167:433–443 e14.
10. Casadevall A. Antibodies to Mycobacterium tuberculosis. *N Engl J Med* 2017;376:283–285.
11. Kondratieva TK, Rubakova EI, Linge IA, Evstifeev VV, Majorov KB, Apt AS. B cells delay neutrophil migration toward the site of stimulus: tardiness critical for effective bacillus Calmette-Guerin vaccination against tuberculosis infection in mice. *J Immunol* 2010;184:1227–34.
12. Turner J, Frank AA, Brooks JV, Gonzalez-Juarrero M, Orme IM. The progression of chronic tuberculosis in the mouse does not require the participation of B lymphocytes or interleukin-4. *Exp Gerontol* 2001;36:537–45.
13. Atzeni F, Batticciotto A, Masala IF, Talotta R, Benucci M, Sarzi-Puttini P. Infections and Biological Therapy in Patients with Rheumatic Diseases. *Isr Med Assoc J* 2016;18:164–7.
14. Liao TL, Lin CH, Chen YM, Chang CL, Chen HH, Chen DY. Different Risk of Tuberculosis and Efficacy of Isoniazid Prophylaxis in Rheumatoid Arthritis Patients with Biologic Therapy: A Nationwide Retrospective Cohort Study in Taiwan. *PLoS One* 2016;11:e0153217.
15. Phuah J, Wong EA, Gideon HP, Maiello P, Coleman MT, Hendricks MR, Ruden R, Cirrincione LR, Chan J, Lin PL, Flynn JL. Effects of B Cell Depletion on Early Mycobacterium tuberculosis Infection in Cynomolgus Macaques. *Infect Immun*

AJRCCM Articles in Press. Published on 21-November-2017 as 10.1164/rccm.201707-1475OC

2016;84:1301–11.
16. Fillatreau S. Novel regulatory functions for Toll-like receptor-activated B cells during intracellular bacterial infection. *Immunol Rev* 2011;240:52–71.
17. Neves P, Lampropoulou V, Calderon-Gomez E, Roch T, Stervbo U, Shen P, Kuhl AA, Loddenkemper C, Haury M, Nedospasov SA, Kaufmann SH, Steinhoff U, Calado DP, Fillatreau S. Signaling via the MyD88 adaptor protein in B cells suppresses protective immunity during Salmonella typhimurium infection. *Immunity* 2010;33:777–90.
18. Shen P, Roch T, Lampropoulou V, O'Connor RA, Stervbo U, Hilgenberg E, Ries S, Dang VD, Jaimes Y, Daridon C, Li R, Jouneau L, Boudinot P, Wilantri S, Sakwa I, Miyazaki Y, Leech MD, McPherson RC, Wirtz S, Neurath M, Hoehlig K, Meinl E, Grutzkau A, Grun JR, Horn K, Kuhl AA, Dorner T, Bar-Or A, Kaufmann SH, *et al.* IL-35-producing B cells are critical regulators of immunity during autoimmune and infectious diseases. *Nature* 2014;507:366–70.
19. Fillatreau S. Cytokine-producing B cells as regulators of pathogenic and protective immune responses. *Ann Rheum Dis* 2013;72 Suppl 2:ii80-4.
20. Rusinova I, Forster S, Yu S, Kannan A, Masse M, Cumming H, Chapman R, Hertzog PJ. Interferome v2.0: an updated database of annotated interferon-regulated genes. *Nucleic Acids Res* 2013;41:D1040-6.
21. Dai P, Wang W, Cao H, Avogadri F, Dai L, Drexler I, Joyce JA, Li XD, Chen Z, Merghoub T, Shuman S, Deng L. Modified vaccinia virus Ankara triggers type I IFN production in murine conventional dendritic cells via a cGAS/STING-mediated cytosolic DNA-sensing pathway. *PLoS Pathog* 2014;10:e1003989.
22. Dey B, Dey RJ, Cheung LS, Pokkali S, Guo H, Lee JH, Bishai WR. A bacterial cyclic dinucleotide activates the cytosolic surveillance pathway and mediates innate resistance to tuberculosis. *Nat Med* 2015;21:401–6.
23. Jin L, Hill KK, Filak H, Mogan J, Knowles H, Zhang B, Perraud AL, Cambier JC, Lenz LL. MPYS is required for IFN response factor 3 activation and type I IFN production in the response of cultured phagocytes to bacterial second messengers cyclic-di-AMP and cyclic-di-GMP. *J Immunol* 2011;187:2595–601.
24. Yang J, Bai Y, Zhang Y, Gabrielle VD, Jin L, Bai G. Deletion of the cyclic di-AMP phosphodiesterase gene (cnpB) in Mycobacterium tuberculosis leads to reduced virulence in a mouse model of infection. *Mol Microbiol* 2014;93:65–79.
25. Schoenen H, Bodendorfer B, Hitchens K, Manzanero S, Werninghaus K, Nimmerjahn F, Agger EM, Stenger S, Andersen P, Ruland J, Brown GD, Wells C, Lang R. Cutting edge: Mincle is essential for recognition and adjuvanticity of the mycobacterial cord factor and its synthetic analog trehalose-dibehenate. *J Immunol* 2010;184:2756–60.
26. Benson SA, Ernst JD. TLR2-dependent inhibition of macrophage responses to IFN-gamma is mediated by distinct, gene-specific mechanisms. *PLoS One* 2009;4:e6329.
27. Fortune SM, Solache A, Jaeger A, Hill PJ, Belisle JT, Bloom BR, Rubin EJ, Ernst JD. Mycobacterium tuberculosis inhibits macrophage responses to IFN-gamma through myeloid differentiation factor 88-dependent and -independent mechanisms. *J Immunol* 2004;172:6272–80.
28. Mayer-Barber KD, Andrade BB, Oland SD, Amaral EP, Barber DL, Gonzales J, Derrick SC, Shi R, Kumar NP, Wei W, Yuan X, Zhang G, Cai Y, Babu S, Catalfamo M, Salazar AM, Via LE, Barry CE 3rd, Sher A. Host-directed therapy of tuberculosis based on interleukin-1 and type I interferon crosstalk. *Nature* 2014;511:99–103.
29. Berry MP, Graham CM, McNab FW, Xu Z, Bloch SA, Oni T, Wilkinson KA, Banchereau R, Skinner J, Wilkinson RJ, Quinn C, Blankenship D, Dhawan R, Cush JJ, Mejias A, Ramilo O, Kon OM, Pascual V, Banchereau J, Chaussabel D, O'Garra A. An interferon-inducible neutrophil-driven blood transcriptional signature in human tuberculosis.

Nature 2010;466:973–7.
30. Cliff JM, Kaufmann SH, McShane H, van Helden P, O'Garra A. The human immune response to tuberculosis and its treatment: a view from the blood. *Immunol Rev* 2015;264:88–102.
31. Chakravarty SD, Zhu G, Tsai MC, Mohan VP, Marino S, Kirschner DE, Huang L, Flynn J, Chan J. Tumor necrosis factor blockade in chronic murine tuberculosis enhances granulomatous inflammation and disorganizes granulomas in the lungs. *Infect Immun* 2008;76:916–26.
32. Li R, Rezk A, Miyazaki Y, Hilgenberg E, Touil H, Shen P, Moore CS, Michel L, Althekair F, Rajasekharan S, Gommerman JL, Prat A, Fillatreau S, Bar-Or A, Canadian B cells in MS Team. Proinflammatory GM-CSF-producing B cells in multiple sclerosis and B cell depletion therapy. *Sci Transl Med* 2015;7:310ra166.
33. Torrado E, Fountain JJ, Robinson RT, Martino CA, Pearl JE, Rangel-Moreno J, Tighe M, Dunn R, Cooper AM. Differential and site specific impact of B cells in the protective immune response to Mycobacterium tuberculosis in the mouse. *PLoS One* 2013;8:e61681.
34. Fillatreau S, Gray D. T cell accumulation in B cell follicles is regulated by dendritic cells and is independent of B cell activation. *J Exp Med* 2003;197:195–206.
35. Fillatreau S, Sweenie CH, McGeachy MJ, Gray D, Anderton SM. B cells regulate autoimmunity by provision of IL-10. *Nat Immunol* 2002;3:944–50.
36. Antonelli LR, Gigliotti Rothfuchs A, Goncalves R, Roffe E, Cheever AW, Bafica A, Salazar AM, Feng CG, Sher A. Intranasal Poly-IC treatment exacerbates tuberculosis in mice through the pulmonary recruitment of a pathogen-permissive monocyte/macrophage population. *J Clin Invest* 2010;120:1674–82.
37. Martinez FO, Gordon S. The M1 and M2 paradigm of macrophage activation: time for reassessment. *F1000Prime Rep* 2014;6:13.
38. Murray PJ, Allen JE, Biswas SK, Fisher EA, Gilroy DW, Goerdt S, Gordon S, Hamilton JA, Ivashkiv LB, Lawrence T, Locati M, Mantovani A, Martinez FO, Mege JL, Mosser DM, Natoli G, Saeij JP, Schultze JL, Shirey KA, Sica A, Suttles J, Udalova I, van Ginderachter JA, Vogel SN, Wynn TA. Macrophage activation and polarization: nomenclature and experimental guidelines. *Immunity* 2014;41:14–20.
39. Rodero MP, Decalf J, Bondet V, Hunt D, Rice GI, Werneke S, McGlasson SL, Alyanakian M-A, Bader-Meunier B, Barnerias C, Bellon N, Belot A, Bodemer C, Briggs TA, Desguerre I, Frémond M-L, Hully M, van den Maagdenberg AMJM, Melki I, Meyts I, Musset L, Pelzer N, Quartier P, Terwindt GM, Wardlaw J, Wiseman S, Rieux-Laucat F, Rose Y, Neven B, *et al.* Detection of interferon alpha protein reveals differential levels and cellular sources in disease. *J Exp Med* 2017;214:1547–1555.
40. Dorhoi A, Yeremeev V, Nouailles G, Weiner J 3rd, Jorg S, Heinemann E, Oberbeck-Muller D, Knaul JK, Vogelzang A, Reece ST, Hahnke K, Mollenkopf HJ, Brinkmann V, Kaufmann SH. Type I IFN signaling triggers immunopathology in tuberculosis-susceptible mice by modulating lung phagocyte dynamics. *Eur J Immunol* 2014;44:2380–93.
41. Joosten SA, van Meijgaarden KE, Del Nonno F, Baiocchini A, Petrone L, Vanini V, Smits HH, Palmieri F, Goletti D, Ottenhoff TH. Patients with Tuberculosis Have a Dysfunctional Circulating B-Cell Compartment, Which Normalizes following Successful Treatment. *PLoS Pathog* 2016;12:e1005687.
42. Wong S-C, Puaux A-L, Chittezhath M, Shalova I, Kajiji TS, Wang X, Abastado J-P, Lam K-P, Biswas SK. Macrophage polarization to a unique phenotype driven by B cells. *Eur J Immunol* 2010;40:2296–2307.
43. McNab FW, Ewbank J, Howes A, Moreira-Teixeira L, Martirosyan A, Ghilardi N, Saraiva M, O'Garra A. Type I IFN induces IL-10 production in an IL-27-independent manner and blocks responsiveness to IFN-gamma for production of IL-12 and bacterial killing in

AJRCCM Articles in Press. Published on 21-November-2017 as 10.1164/rccm.201707-1475OC

Mycobacterium tuberculosis-infected macrophages. *J Immunol* 2014;193:3600–12.
44. O'Garra A, Redford PS, McNab FW, Bloom CI, Wilkinson RJ, Berry MP. The immune response in tuberculosis. *Annu Rev Immunol* 2013;31:475–527.
45. Manca C, Tsenova L, Freeman S, Barczak AK, Tovey M, Murray PJ, Barry C, Kaplan G. Hypervirulent M. tuberculosis W/Beijing strains upregulate type I IFNs and increase expression of negative regulators of the Jak-Stat pathway. *J Interferon Cytokine Res* 2005;25:694–701.
46. Ordway D, Henao-Tamayo M, Harton M, Palanisamy G, Troudt J, Shanley C, Basaraba RJ, Orme IM. The hypervirulent Mycobacterium tuberculosis strain HN878 induces a potent TH1 response followed by rapid down-regulation. *J Immunol* 2007;179:522–31.
47. Maertzdorf J, Weiner J 3rd, Mollenkopf HJ, Network TB, Bauer T, Prasse A, Muller-Quernheim J, Kaufmann SH. Common patterns and disease-related signatures in tuberculosis and sarcoidosis. *Proc Natl Acad Sci U A* 2012;109:7853–8.
48. Knaul JK, Jorg S, Oberbeck-Mueller D, Heinemann E, Scheuermann L, Brinkmann V, Mollenkopf HJ, Yeremeev V, Kaufmann SH, Dorhoi A. Lung-residing myeloid-derived suppressors display dual functionality in murine pulmonary tuberculosis. *Am J Respir Crit Care Med* 2014;190:1053–66.
49. Lampropoulou V, Hoehlig K, Roch T, Neves P, Calderon Gomez E, Sweenie CH, Hao Y, Freitas AA, Steinhoff U, Anderton SM, Fillatreau S. TLR-activated B cells suppress T cell-mediated autoimmunity. *J Immunol* 2008;180:4763–73.
50. Tomasello E, Pollet E, Vu Manh T-P, Uzé G, Dalod M. Harnessing Mechanistic Knowledge on Beneficial Versus Deleterious IFN-I Effects to Design Innovative Immunotherapies Targeting Cytokine Activity to Specific Cell Types. *Front Immunol* 2014;5:526.

Legends to Figures

Figure 1. B cells from Mtb-infected mice display a STAT1 signature. A) Heatmap of the differentially expressed genes [selected on the basis of an adjusted p-value (Benjamini Hochberg procedure) < 0.05 and a fold change > 2 or < 0.5] both between B cells from the spleen of naive C57BL/6 mice and B cells from the spleen of Mtb-infected mice on the one side, as well as between B cells from the spleen of naive C57BL/6 mice B cells from the lung of infected mice after 21 days of infection one the other side (we had to pool the B cells from three independent mice in order to obtain the necessary amount of mRNA to perform a microarrays and 4 to 5 independent microarrays were performed for each of the 3 conditions indicated above). The color key for the red and blue colors is indicated. B) Main network deduced from the Ingenuity Pathway Analysis involved in B cells from Mtb-infected lungs and spleens, as compared to naive spleens. Full lines and dotted lines indicate direct and indirect interactions, respectively. Differentially expressed genes present in the pathways are represented in red. Pale red: 2 < fold change <10; dark red fold change >10. C) RT-qPCR analysis of mRNA expression of the *Stat1, Irgm1* and *Csf1* genes found to be up-regulated in the transcriptome of B cells purified from the spleen of naive mice or from spleen and lung of Mtb-infected C57BL/6 mice (for each sample, B cells were pooled from 3 independent mice. 4-5 independent infection experiments were performed). D) As in C) except that the *Ccrl2, Ccl5* and *Cxcl9* genes were analyzed. Data represent mean±s.e.m. and were analyzed by the two-tailed Mann-Whitney test. * P≤0.05; ** P≤0.01; *** P≤0.001.

Figure 2. B cells from Mtb-infected mice produce and respond to type I IFN. A) The Venn diagram shows the differentially expressed genes known to be regulated by type I, type II and/or type III IFN according to Interferome analysis. The histogram on the right indicates

AJRCCM Articles in Press. Published on 21-November-2017 as 10.1164/rccm.201707-1475OC

the relative expression of the five genes regulated only by type I IFN in B cell samples from naive spleen or Mtb-infected spleen or lungs (microarray data). B) B cells purified from the spleen of naive C57BL/6 mice were stimulated for 24h with IFNα or not, and the mRNA expression of IFN stimulated genes was analyzed by RT-qPCR (n=3). C) Overlay of flow cytometry histograms showing phospho-STAT1 staining in lung B cells from Mtb-infected mice stimulated for 15 min with IFNα (n=3, a representative experiment out of 2 independent experiments is shown). D) Expression of *Ifnb*, *Il6* and *Il10* in B cells purified from the spleen of naive (NS) or Mtb-infected (IS) C57BL/6 mice and from the lungs of Mtb-infected (IL) C57BL/6 mice after 21 days of infection (for each sample, B cells were pooled from 3 independent mice. 4-5 independent infection experiments were performed) E) *Ifna* mRNA induction in B cells purified from naive C57BL/6 spleens upon *in vitro* 24h stimulation or not with Mtb [multiplicity of infection (MOI)=0.3); n=12]. F) As in E) except that *Ifnb* mRNA induction was measured (n=12). G) Activity of type I IFN measured using a reporter assay in the supernatant of naive splenic B cells stimulated or not for 6 days with Mtb (MOI=0.3; n=8 independent preparations of B cells per group). H) Concentrations of IFNβ measured by ELISA in the supernatants of naive splenic B cells stimulated for 6 days or not with Mtb (MOI=0.3; n=13 independent preparations of B cells per group). I) *Ifnb* mRNA expression in B cells purified from the spleen of WT or *Ifnar1*$^{-/-}$ mice upon *in vitro* stimulation for 24h with Mtb (MOI=0.3); fold change is relative to respective expression before stimulation (n=5). J) *Ifnb* mRNA expression in B cells purified from the spleen of C57BL/6 mice upon *in vitro* stimulation (supMtb) for 24h or not (7H9 medium) with Mtb-culture supernatant (n=7). Data represent mean±s.e.m. and were analyzed using the non-parametric two-tailed Mann-Whitney test or the Wilcoxon test (A, B, D, G, I) * P≤0.05; ** P≤0.01; *** P≤0.001. For E, F, H and J we used the parametric two-tailed Student's paired *t*-test (# P≤0.05; ## P≤0.01; ### P≤0.001).

Figure 3. STING and its ligand trigger type I IFN expression in B cells. A) *Ifnb* mRNA expression in B cells purified from the spleen of WT (black bars) or *Sting*$^{-/-}$ (white bars) upon stimulation for 24h with Mtb (MOI=0.3); fold change represents expression after 24h of stimulation relative to respective expression before stimulation (n=5 to 10 mice per group). B) Concentration of IFNβ in the supernatants of naive splenic B cells from WT or *Sting*$^{-/-}$ mice stimulated for 6 days or not with Mtb (n= 4 per group). C) *Ifnb* mRNA expression in B cells purified from the spleen of naive WT (black bars) or *Sting*$^{-/-}$ (white bars) mice stimulated (+) or not (-) with c-di-AMP during 24h (n=4 per group). D) Concentration of IFNβ in the supernatants of naive splenic B cells from WT or *Sting*$^{-/-}$ mice stimulated for 3 days or not with c-di-AMP (n= 5 per group). E) *Ifnb* mRNA expression in CD21^{low}CD23^{hi} follicular (FO), CD21^{hi}CD23^{low} marginal zone (MZ) and CD21^{-}CD23^{-} double-negative (DN) B cells sorted from the spleen of naive C57BL/6 mice upon 24h stimulation (+) or not (-) with c-di-AMP; fold change is relative to unstimulated follicular B cells (n=3). Each symbol represents B cells purified from individual mouse. F) Concentration of IFNβ in the supernatants of CD19^{+} and CD19^{-} lung cells purified from Mtb-infected C57BL/6 mice upon 24h *ex vivo* stimulation (+) or not (-) with c-di-AMP (for each sample, B cells were pooled from 3 independent mice and we performed 4-5 independent infection experiments). G) *Ifnb* mRNA expression in splenic B cells from WT mice stimulated or not with the indicated TLR ligands during 24h (n= 4-7). H) Concentration of IFNβ in the supernatants of splenic B cells from WT mice stimulated or not with the indicated TLR ligands during 3 days (n= 4 per group). Data represent mean±s.e.m. and were analyzed using the two-tailed (A,C,E,F,G,H) or one-tailed (B, D) Mann-Whitney test. * P≤0.05; ** P≤0.01; *** P≤0.001. One-tailed Mann-Whitney was used in panels B and D since protein expression is expected to positively correlate with mRNA expression.

AJRCCM Articles in Press. Published on 21-November-2017 as 10.1164/rccm.201707-1475OC

Figure 4. MyD88 signaling negatively regulates type I IFN expression in B cells. A) *Ifnb* mRNA expression in B cells purified from the spleen of *Myd88*$^{-/-}$ (white bars) and WT (black bars) control mice upon stimulation for 24h with Mtb (MOI=0.3); fold change represents expression after stimulation relative to respective expression before stimulation (set to 1) (n=10 mice per group). B) Concentration of IFNβ in the supernatants of naive splenic B cells from WT or *Myd88*$^{-/-}$ mice stimulated for 6 days or not with Mtb (n=3). C-E) *Ifnb* mRNA expression in B cells purified from the spleen of WT mice (n=4-8 mice per group) upon 24h *in vitro* stimulation with either c-di-AMP (C), TDB (D) or Mtb (E) in the presence (+) or absence (-) of the TLR2 agonist Pam_3CSK_4. F) B cells from WT mice were stimulated with c-di-AMP and/or IL1β then IFNβ expression was analyzed at the mRNA level (n= 6). G) As in F) except that *Myd88*$^{-/-}$ B cells were used (n= 4). Data represent mean±s.e.m. and were analyzed by using the two-tailed Mann-Whitney test or the two-tailed Wilcoxon test (B-E) (* P≤0.05; ** P≤0.01; *** P≤0.001). The two-tailed Student's paired t-test was used for A and F (# P≤0.05; ## P≤0.01; ### P≤0.001).

Figure 5. Expression of IFNβ in blood B cells from healthy donors after Mtb stimulation and in pleural B cells of TB patients. A) Induction of *IFNB* mRNA expression in peripheral blood B cells of healthy donors stimulated or not for 24h with Mtb (MOI=0.3; n=8). B) *IFNA* mRNA expression in B cells purified from peripheral blood mononuclear cells (PBMC) of healthy donor as in A) (n=8). C) *IFNB* mRNA expression in B cells purified from the blood of healthy donors stimulated (+) or not (-) with c-di-AMP for 24h (n=4 per group). D-F) mRNA expression of *IFNB* (D), *BST2* (E) and *CXCL10* (F) in B cells from peripheral blood of healthy donors, TB patients, and in B cells from pleural fluid of TB patients. Each symbol represents an independent donor (n=6-7 individuals per group). The expression level was arbitrarily set to 1 for one sample from the peripheral blood of healthy donors group, and the

values for the other samples were calculated relatively to this reference. Data represent mean±s.e.m. and were analyzed using the two-tailed Mann-Whitney test or the two-tailed Wilcoxon test (*P≤0.05; ** P≤0.01; *** P≤0.001) except for panel A, B and F where a two-tailed Student's paired *t*-test was used (# P≤0.05; ## P≤0.01; ### P≤0.001).

Figure 6. IFNβ production by B cells polarizes macrophages *in vitro* toward an anti-inflammatory phenotype. A) *Cox2*, *Nos2* and *Ym1* mRNA expression in WT macrophages first conditioned or not with supernatant of *Mtb*-stimulated B cells, and then infected with Mtb (MOI=0.5; n=6 to 7). B) Same as in A) but in WT or *Ifnar1*$^{-/-}$ macrophages. (MOI=0.5; n=4). C) Overlay of flow cytometry histograms and D) mean fluorescence intensity (MFI) of PD-L1 surface expression on macrophages from the bone marrow of naive WT or *Ifnar1*$^{-/-}$ mice and incubated (supB) or not (Ctrl) for 24h with supernatants of Mtb-stimulated B cells (n=4 independent preparations of B cells per group). E) *CCL2* mRNA expression in human monocyte-derived macrophages incubated with supernatants of human B cells stimulated or not with Mtb (n=4). F) Overlay of flow cytometry histograms and cumulative geometric mean fluorescence intensity (MFI) representing PD-L1 surface expression on macrophages incubated with supernatants of B cells stimulated or not with Mtb (n=4). Results were analyzed using the two-tailed Mann-Whitney test or the two-tailed Wilcoxon test (*P≤0.05; ** P≤0.01; *** P≤0.001) except for panel A where a two-tailed Student's paired *t*-test was used (# P≤0.05; ## P≤0.01; ### P≤0.001).

Figure 7. Excessive production of type I IFN by B cells is associated with altered macrophage polarization and reduced inflammation in the lungs of Mtb-infected mice. Mixed bone marrow chimeras were generated in which B cells were competent (B-WT, i.e. 80% μMT + 20%WT→ WT, black bars) or deficient (B-*Myd88*$^{-/-}$, i.e. 80% μMT + 20%

AJRCCM Articles in Press. Published on 21-November-2017 as 10.1164/rccm.201707-1475OC

Myd88$^{-/-}$ →WT, white bars) for *Myd88*. B-CTRL mice (80% WT + 20% *MyD88*$^{-/-}$→WT) lacking *Myd88* expression on 20% total hematopoietic cells were also used as control. These mice were infected with 1000 CFUs Mtb, H37Rv strain, and their lungs analyzed 6 weeks later. A) *Ifnb* mRNA expression in B cells purified from the lungs of Mtb-infected B-WT and B-*Myd88*$^{-/-}$ mice (for each sample, B cells were pooled from 3 independent mice and we performed 5 independent infection experiments). The expression level was arbitrarily set to 1 for one sample from the B-*Myd88*$^{-/-}$ group, and the values for the other samples were calculated relatively to this reference. B) Representative dot plot of CD11b *vs*. Gr-1 staining in the lungs of B-WT or and B-*Myd88*$^{-/-}$ mice infected for 42 days with Mtb. The gates indicate the percentage of CD11b^{int}Gr-1^{int} cells among total lung cells. One representative experiment out of two independent experiments is shown. C) Percentage of Gr1^{int}CD11b^{int} cells in the lung of B-WT or B-*Myd88*$^{-/-}$ mice (n=7). D) CD11b^{+}Gr1^{-} (Mf) and CD11b^{int}Gr1^{int} cells were sorted by FACS from the lungs of C57BL/6 mice infected with Mtb for 42 days and then analyzed for the expression of the indicated genes (n=5). E) mRNA expression of pro-inflammatory cytokines and anti-inflammatory genes in the lung of B-WT and B-*Myd88*$^{-/-}$ mice (n=3). Data represent mean±s.e.m., are representative of two independent experiments, and were analyzed using the two-tailed Mann-Whitney test. *P≤0.05; ** P≤0.01; *** P≤0.001 except for panel C where a two-tailed Student's paired *t*-test (# P≤0.05; ## P≤0.01; ### P≤0.001).

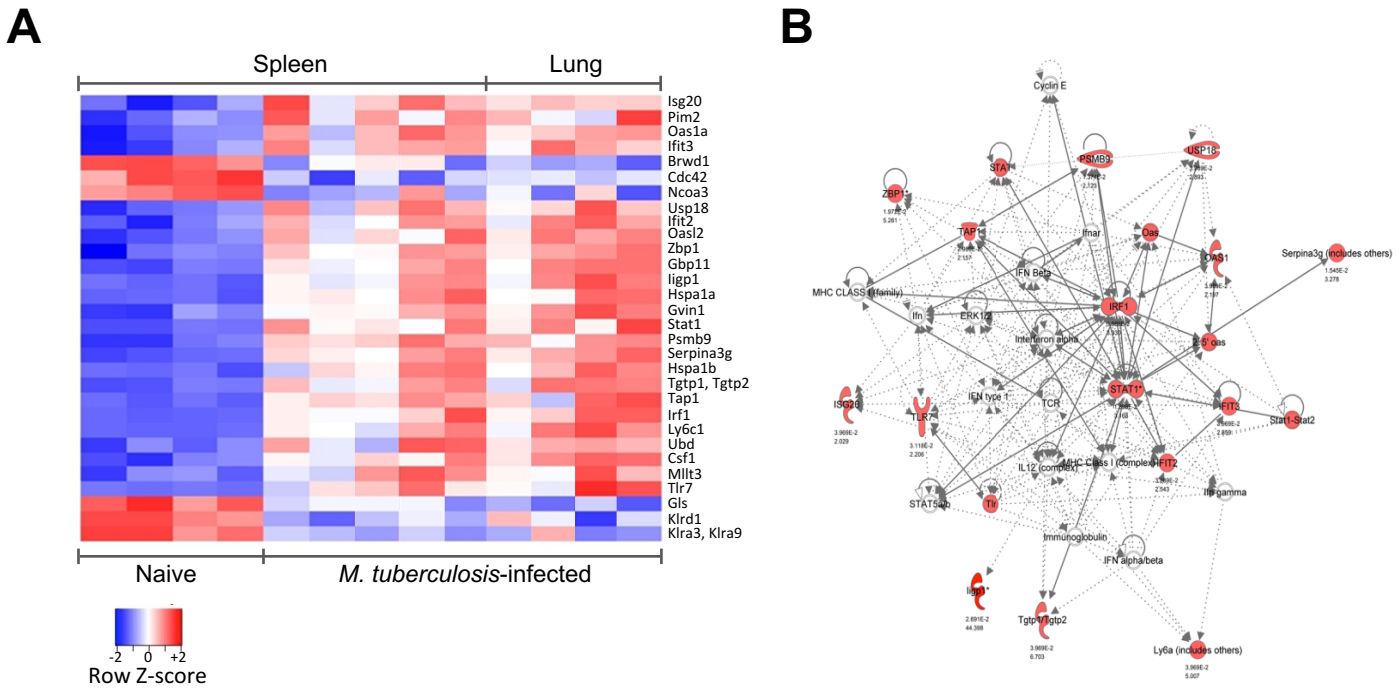

Figure 1

AJRCCM Articles in Press. Published on 21-November-2017 as 10.1164/rccm.201707-1475OC

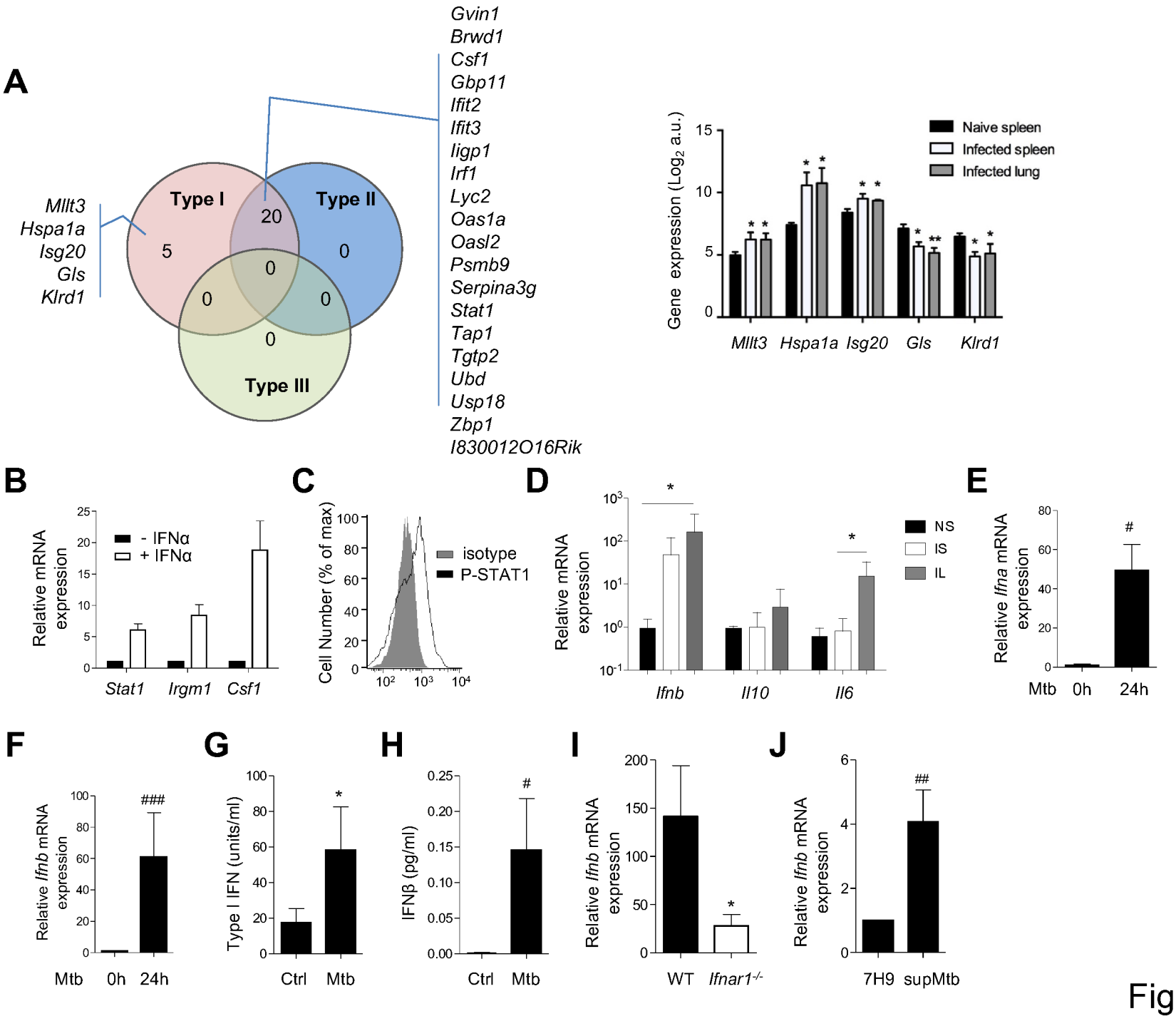

Figure 2

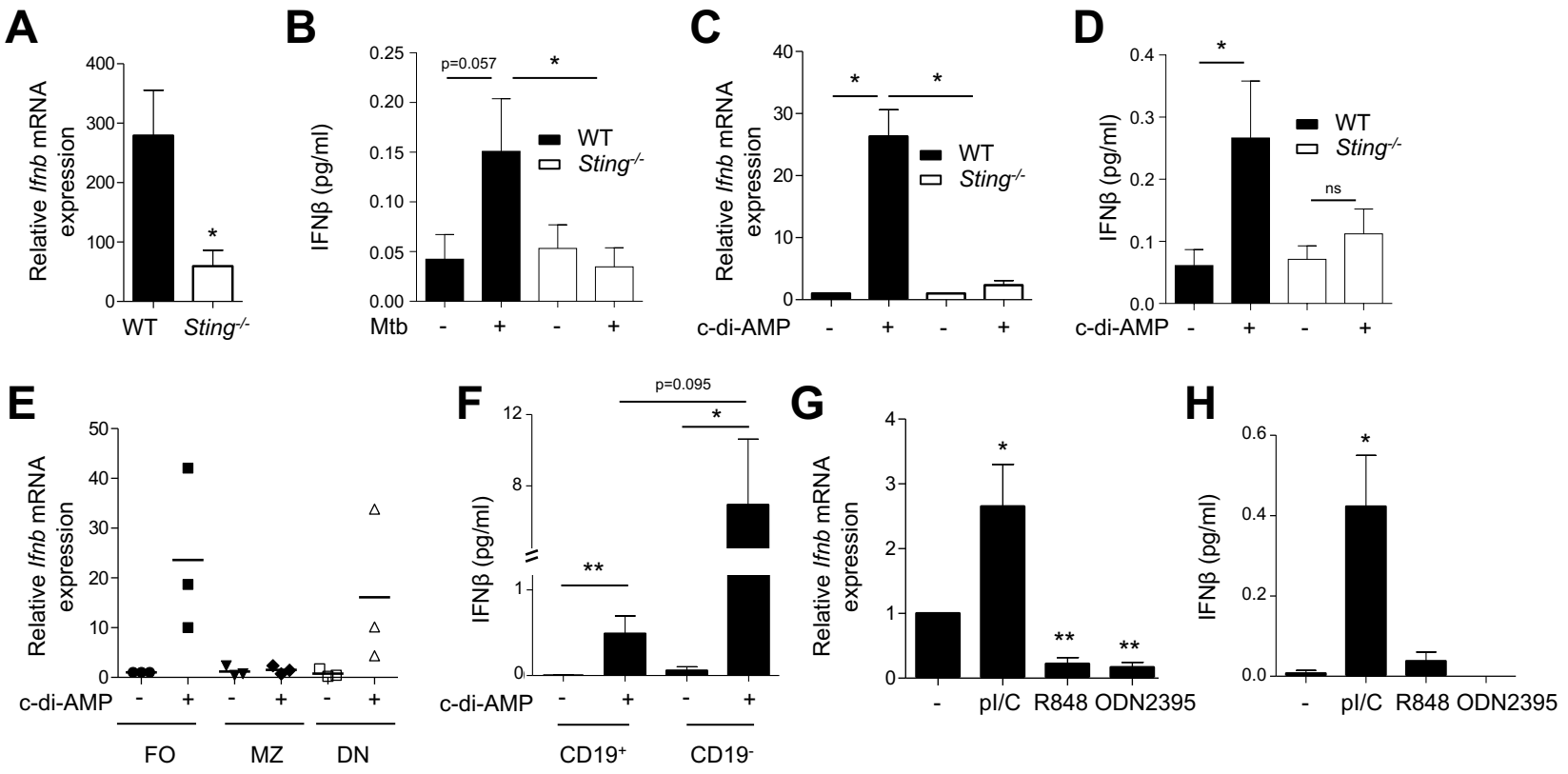

Figure 3

AJRCCM Articles in Press. Published on 21-November-2017 as 10.1164/rccm.201707-1475OC

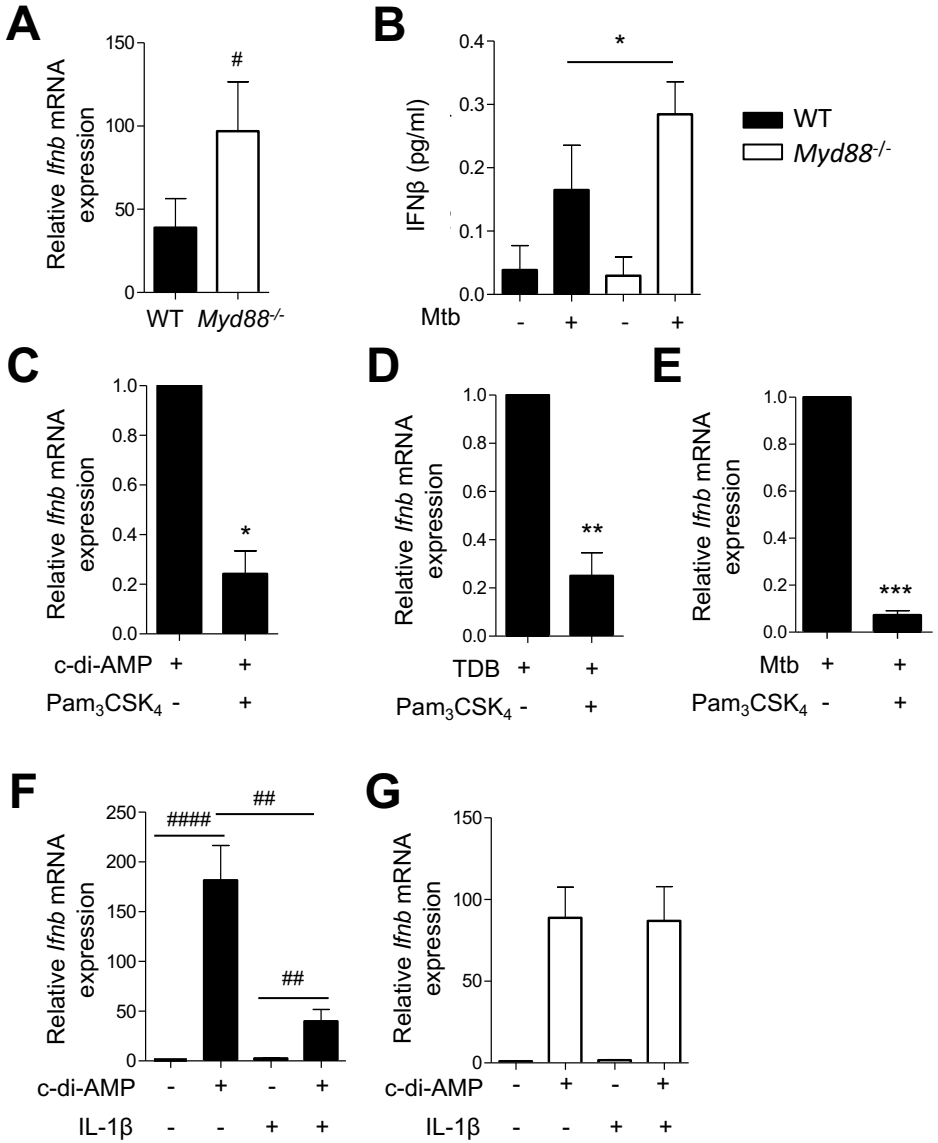

Figure 4

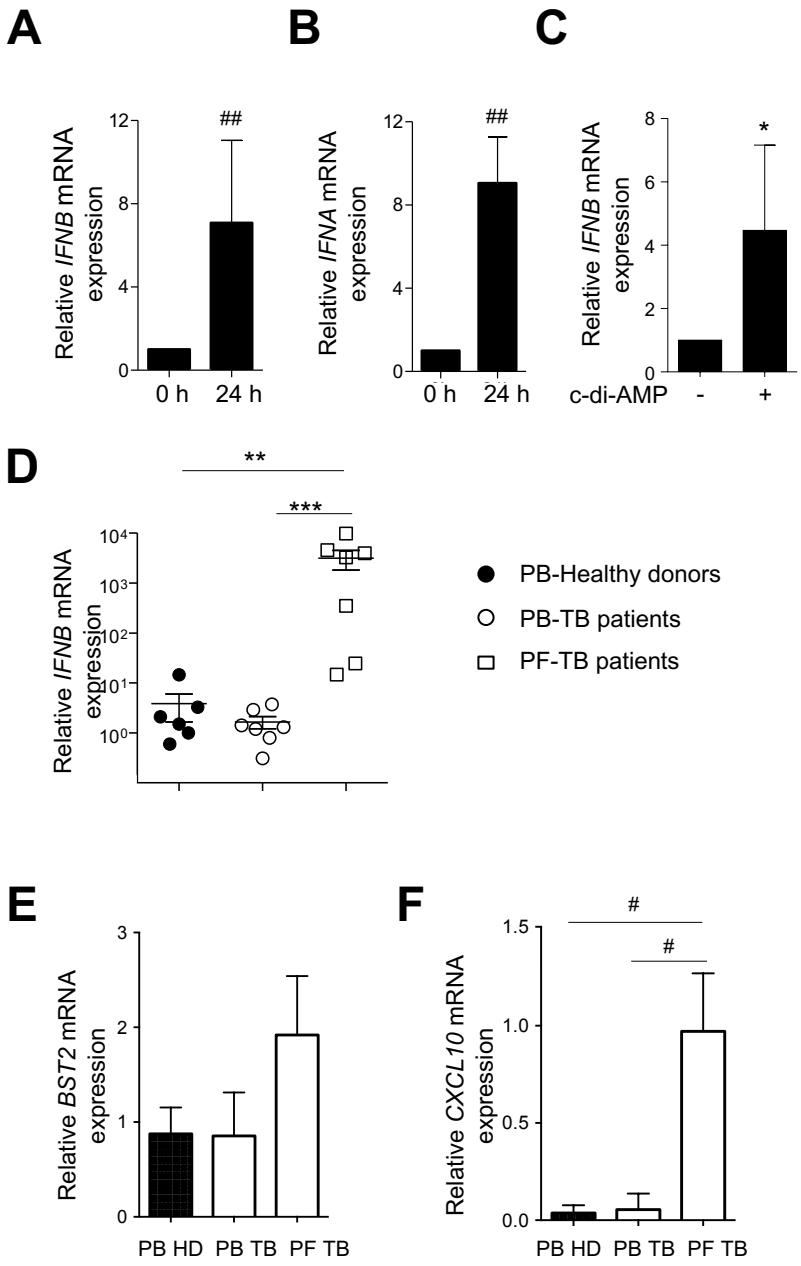

Figure 5

AJRCCM Articles in Press. Published on 21-November-2017 as 10.1164/rccm.201707-1475OC

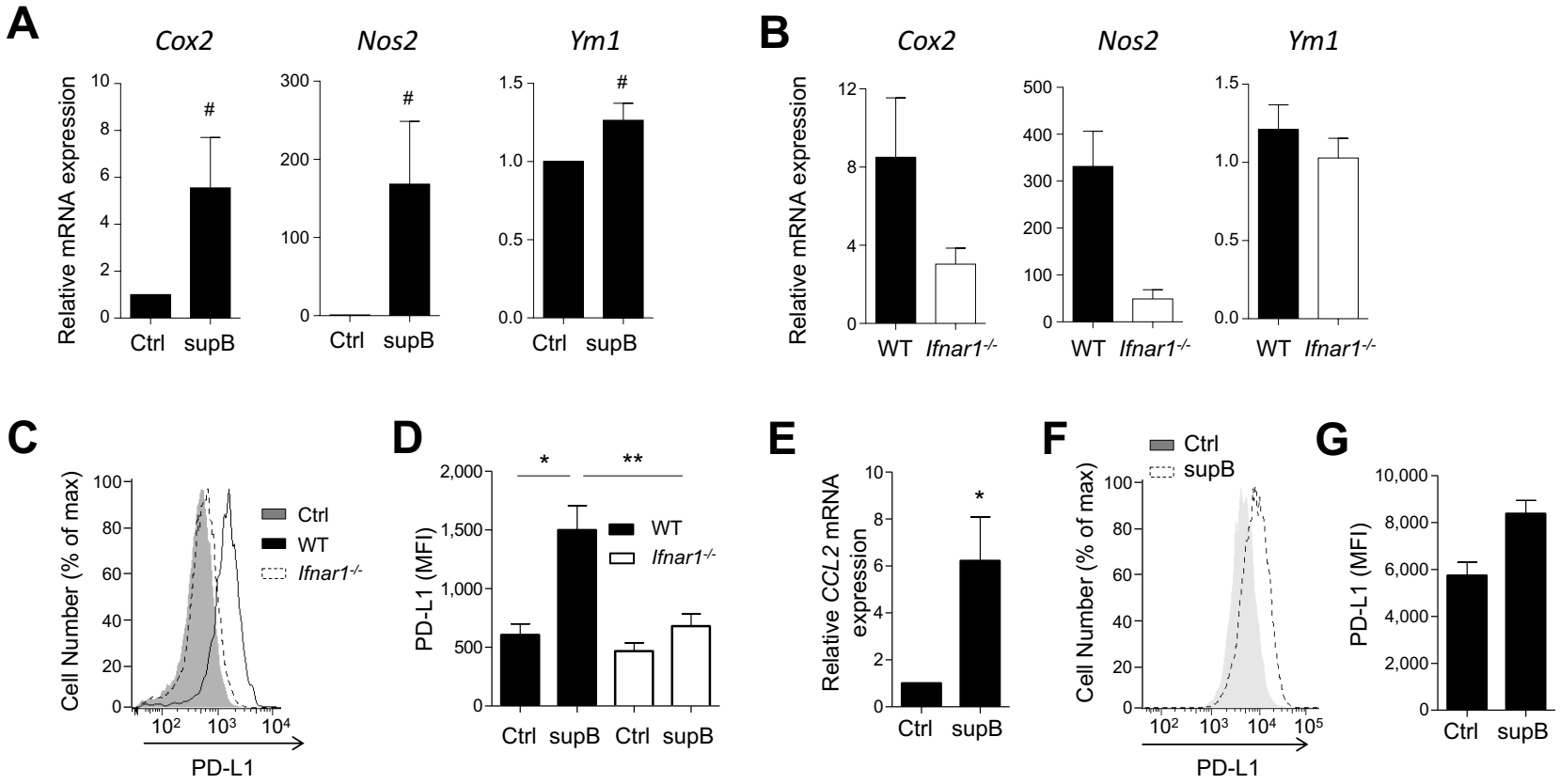

Figure 6

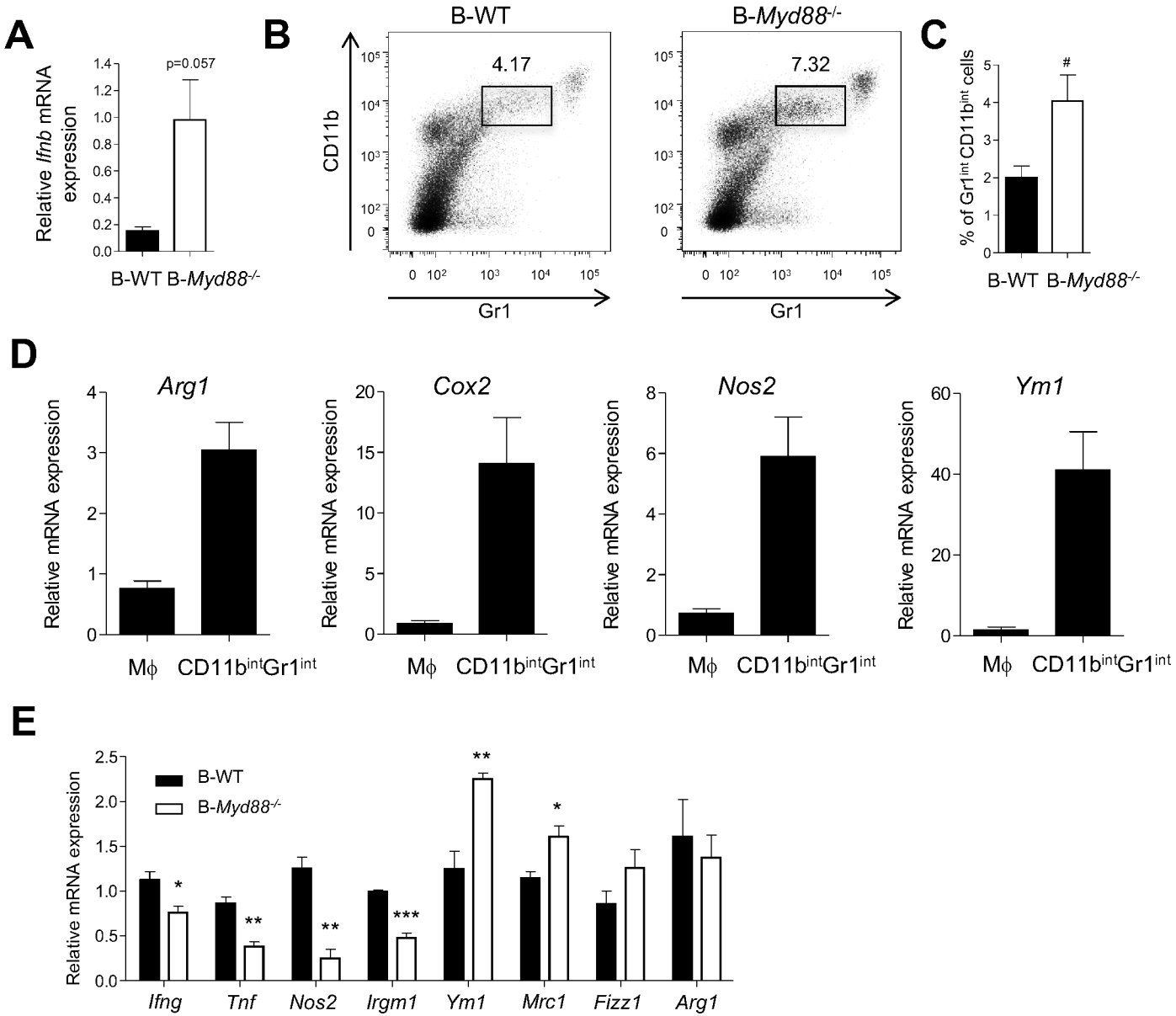

Figure 7

AJRCCM Articles in Press. Published on 21-November-2017 as 10.1164/rccm.201707-1475OC

Online Data Supplement

B cells producing type I interferon modulate macrophage polarization in tuberculosis

Alan Bénard, Imme Sakwa, Pablo Schierloh, André Colom, Ingrid Mercier, Ludovic Tailleux, Luc Jouneau, Pierre Boudinot, Talal Al-Saati, Roland Lang, Jan Rehwinkel, Andre G. Loxton, Stefan H. E. Kaufmann, Véronique Anton-Leberre, Anne O'Garra, Maria Del Carmen Sasiain, Brigitte Gicquel, Simon Fillatreau, Olivier Neyrolles, Denis Hudrisier

Supplemental methods

TB Patients. TB patients with or without moderate and large pleural effusions were identified at the Servicio de Tisioneumonología. Physical examination, complete blood cell count, electrolytes, chest X-ray, human immunodeficiency virus (HIV) test, adenosine deaminase and lactate dehydrogenase in PF were performed. The diagnosis of tuberculous pleurisy was based on a positive Ziehl–Neelsen stain or Lowenstein–Jensen culture from PF and/or histopathology of pleural biopsy, and was confirmed further by an Mtb-induced IFN-γ response and an adenosine deaminase-positive test. Exclusion criteria included a positive HIV test or the presence of concurrent infectious diseases. PFMC and PBMC samples were obtained by Ficoll-Hypaque gradient and stored frozen in liquid N_2 until B cell isolation.

Mixed BM chimera. Mixed bone-marrow chimera mice were prepared as previously described [15]. Briefly, for the generation of mice lacking *Myd88* in B cells, C57BL/6 WT mice were lethally irradiated (950 rads) using a γ-irradiator BioBeam 8000 and reconstituted with a total of $5x10^6$ donor derived bone-marrow cells (depleted in NK and T cells by complement-mediated lysis using anti-Thy1 and anti-NK1.1 mAb) from B cells-deficient mice (μMT) mixed at ratio 4/1 with bone-marrow cells from MyD88-deficient mice. WT mice receiving a mixture of μMT and *Myd88*$^{-/-}$ BM cells (μMT + *Myd88*$^{-/-}$ →WT) lack *Myd88* in B cells and in 20% of non-B cells and were termed "B-*Myd88*$^{-/-}$". To control for the effect due to the lack of

Myd88 in 20% non-B cells, control chimeric mice in which irradiated WT recipient mice received a mixture of WT and *Myd88*$^{-/-}$ BM cells (WT + *Myd88*$^{-/-}$ →WT) served as a control. These mice lacked *Myd88* in 20% of B and non-B cells and were named B-CTRL mice. Irradiated WT mice reconstituted with a mixture of μMT and WT BM cells (μMT + WT →WT) expressed *Myd88* in all cells including B cells and were termed "B-WT". Chimeric mice were treated with broad spectra antibiotics (Bactrim, Roche, Bâle, Switzerland) in the drinking water until full reconstitution of the hematopoietic system (6-8 weeks).

Culture of Mtb. Mtb (H37Rv strain) was grown at 37 °C in Middlebrook 7H9 medium (Difco Livonia, MI) supplemented with 10% albumin-dextrose-catalase supplement (Difco) and 0.05% Tween-80 (Sigma-Aldrich, St. Louis, MO) or on Middlebrook 7H11 agar medium (Difco) supplemented with 10% oleic acid-albumin-dextrose-catalase supplement (OADC, Difco). All cultures were performed in a BSL3 laboratory.

Mouse infection. Six- to eight-week-old female C57BL/6 mice or chimeric mice were anesthetized with a cocktail of ketamine (100 mg/kg; Merial, Lyon, France) and xylasine (15 mg/kg; Bayer, Leverkusen, Germany) and infected intranasally with ≈1,000 CFUs of Mtb H37Rv (dissociated by repeated passage through G-25 and G-26 needles) in 25 μl of saline/0.01% Tween 80. After the indicated period of time (usually 21 and 42 days), mice were sacrificed by cervical dislocation and their lungs and spleens were collected and homogenized using a gentleMACS Tissue Dissociator (Miltenyi Biotech) before used in *in vitro* assays, or for subsequent isolation of immune cell subsets.

Scoring of CFUs. To determine the bacterial burdens in the lungs and spleens of infected animals, 100 μl of a 4-ml homogenate of lungs or spleen were plated in serial dilutions onto 7H11-OADC agar medium, and CFU scoring was done after 3 weeks of incubation at 37°C.

Histological analysis. Infected mice were euthanized by cervical dislocation. Lungs were removed, immediately fixed in JB fixative (zinc acetate 0.5%, zinc chloride 0.05%, and

AJRCCM Articles in Press. Published on 21-November-2017 as 10.1164/rccm.201707-1475OC

calcium acetate 0.05% in Tris buffer at pH 7) for 7 days and then embedded in low–melting point paraffin (Poly Ethylene Glycol Distearate; Sigma). Sections were cut (3 μm) and stained with hematoxylin and eosin for histological lesion description. Blind scoring was performed by a pathologist.

Isolation of B cells. For *ex vivo* studies in the mouse, lungs and spleens from Mtb-infected mice were ground using a gentleMACS Tissue Dissociator. Collagenase (2.5 mg/ml, Roche) and DNAse (100 U/ml, Roche) were added for 30 min at 37°C to lung samples to improve cell recovery. B cells were purified by positive magnetic selection using anti-CD19 microbeads, according to the manufacturer's instructions with two subsequent passages on the columns (Miltenyi Biotec). Purity was >95%.

For *in vitro* studies, the spleens of naive mice were ground using a gentleMACS Tissue Dissociator. Cell suspension was depleted for red blood cells and filtered (30 μm, Miltenyi Biotec). B cells were purified by negative selection using a mix of CD43 and CD11c microbeads (Miltenyi Biotec) (purity >95%) or were sorted by FACS for the analysis of B cell subpopulations.

Peripheral blood B cells from healthy donors were purified by positive selection using anti-CD19 microbeads. Pleural Fluid (PF) or peripheral blood B cells from TB patients were positively selected as previously reported[27]. Briefly, ≈2×10^7 PFMC or PBMC were incubated at 4°C for 30 min using anti-CD19 mAb. Then, magnetic selection was performed using anti-mouse IgG microbeads according to the manufacturer's instructions (Miltenyi Biotec). This procedure yielded a purity >95%.

B cells stimulation *in vitro*. Purified B cells were cultured in RPMI-1640 GlutaMax supplemented with 10% fetal calf serum (FCS, Pan-Biotech, Aidenbach, Germany), 50 μM of β-mercaptoethanol and 1 mM of sodium pyruvate at 37°C in the presence of 5% CO2. B cells were stimulated for the indicated period of time (in 12-well plates at $2x10^6$ cells/well for *in*

vitro assay or at 10^6 cells/well for *ex vivo* assay) by H37Rv at a multiplicity of infection (MOI) of 0.3 bacteria/cell, c-di-AMP (10 µg/ml) (Invivogen, Toulouse, France), TDB (10 µg/ml, Invivogen), Pam_3CSK_4 (5 µg/ml, Invivogen), recombinant IFNα (10 ng/ml, PBL Assay Science, Piscataway, NJ), or H37Rv culture supernatants (10% of cells volume). Then B cells were treated in TRIzol (Life Technologies) for mRNA analysis, or stained with mAb for phenotypic analysis, or their supernatants were collected and double-filtrated for cytokine measurement or macrophage conditioning.

Macrophage differentiation and conditioning. Murine BM cells were flushed out of the femurs and tibias of 6- to 8-week-old female C57BL/6 mice and cultured in Petri dishes (2×10^6 cells per dish). For human macrophages, peripheral blood samples were obtained from healthy donors through the Etablissement Français du Sang (Toulouse, France). Then, peripheral blood mononuclear cells (PBMC) were isolated by Ficoll density gradient (GE Healthcare, Little Chalfont, UK). Monocytes were then purified from freshly isolated PBMC by positive magnetic selection using anti-CD14 microbeads (Miltenyi Biotec), according to the manufacturer's instructions.

Murine bone-marrow cells and human monocytes were cultured in RPMI-1640 GlutaMax (Life Technologies, Carlsbad, CA) supplemented with 10% FCS, 50 µM β-mercaptoethanol (Life Technologies), 1 mM sodium pyruvate (Life Technologies) and 20 ng/ml M-CSF (PeproTech, Rocky Hill, NJ) at 37°C in the presence of 5% CO2. Medium was supplemented with fresh medium containing 20 ng/ml of M-CSF after three days of culture. Macrophages differentiated *in vitro* in the presence of M-CSF were stimulated with supernatants from Mtb-stimulated B cells or control supernatants for the indicated periods of time at $6x10^5$ cells per well in 12-well plates. Cells were collected for cytometry using cell dissociation buffer (Sigma-Aldrich) or lysed by TRIzol for RNA extraction. For cytokine stimulation,

AJRCCM Articles in Press. Published on 21-November-2017 as 10.1164/rccm.201707-1475OC

conditioned macrophages were infected with H37Rv (MOI = 0.5) for 18 hours and supernatants were collected and double-filtered (0.22 μm; MERK, Kenilworth, NJ).

Microarray hybridization and data analysis. cRNA were hybridized on Affymetrix GeneChip® Mouse Genome 430 2.0 arrays, using standard Affymetrix protocol after quality control with Agilent 2100 Bioanalyzer and quantification with NanoDrop ND-1000 spectrophotometer, as previously described (52). The significantly differentially regulated genes were detected using a *t*-test based R-script, with p values adjusted using Benjamini Hochberg procedure. In order to be selected in a comparison of two conditions, each Affy ID had to fulfill the following criteria: (i) be present in at least three of the four arrays for at least one of the two conditions compared, (ii) have a mean signal intensity higher than 50 in at least one of the two conditions, and (iii) show an adjusted p-value <0.05 (*t*-test) in the comparison of the two conditions. The genes differentially expressed between X- and Y cells (*t*-test; $p<0.05$) were then selected and filtered using the gene ontology resource (www.geneontology.org). Hierarchical clustering was performed with the MeV program (version 4.8.1.30) using Pearson correlation and average Linkage. Data were analyzed through the use of QIAGEN's Ingenuity® Pathway Analysis (IPA®, QIAGEN Redwood City,www.qiagen.com/ingenuity) and using the Interferome Database (http://interferome.its.monash.edu.au/interferome/home.jspx) (21). The row z-score was obtained by subtracting the mean of the row from every value and then dividing the resulting values by the standard deviation of the row.

Quantitative RT-PCR. Real-time PCR was performed as previously described (53). Briefly, RNA was extracted from cells by guanidine-isothiocyanate-phenol-chloroform using ready-to-use TRIzol or by RNeasy mini kit (Qiagen, Venlo, Netherlands). Complementary DNA was reverse transcribed from 1 μg total RNA with Moloney murine leukemia virus reverse transcriptase (Life Technologies) using random hexamer oligonucleotides for priming (Life

Technologies). The amplification was performed with an ABI Prism 7500 Sequence Detector (Life Technologies) using the PCR SYBR Green sequence detection system (Eurogentec, Seraing, Belgium). Data were analyzed using the software supplied with the Sequence Detector (Life Technologies). The mRNA content was normalized to the hypoxanthine-guanine phosphoribosyltransferase (*Hprt*) mRNA for mouse genes and metastatic lymph node protein 51 (*MLN51*) or cyclophilin D (*CYLD*) mRNA for human genes. Gene expression was quantified using the ΔΔCt method. Primers are listed in Supplementary Table 2 and Supplementary Table 3.

Flow cytometry. Flow cytometry was performed using a LSR-II cytometer (BD Bioscience) or a MacsQuant analyser (Miltenyi Biotec). The anti-human antibodies were directed against PDL1 (29E.2.A3) and CD19 (4G7). The anti-mouse antibodies were directed against B220 (RA3-6B2), CD4 (RM4-5), CD8α (53-6.7), CD21 (B3B4), CD23 (7G6), CD11b (M1/70), Gr1 (RB6-8C5), PDL1 (10F.9G2) and phospho-STAT1 (4a). Antibodies were purchased from BD Bioscience (San Jose, CA), eBioscience (San Diego, CA) or BioLegend (San Diego, CA). For phospho-STAT1 staining, lung homogenates were stimulated by recombinant IFNα (10^5 U/ml) during 15 minutes at 37°C, fixed for 30 minutes (BD Cytofix, BD Bioscience) at 4°C, washed with PBS 1% BSA, permeabilized for 30 minutes (BD Phosflow Perm Buffer III, BD Bioscience) at 4°C, washed with PBS 1% BSA, stained with antibodies for 30 min at 4°C and washed two times with PBS. All data were analyzed with the FlowJo software (Ashland, OR). For sorting of B cell subpopulations, live B cells were stained using anti-CD19, -CD21 and -CD23 mAb and were separated via FACS into $CD21^+CD23^+$, $CD21^{hi}CD23^{low}$ and $CD21^-CD23^-$ fractions.

Cytokine detection. Secreted cytokines were measured by ELISA assays using kits from BD Bioscience (IL-10, IFNγ), Biolegend (IL1β) and PBL Assay Science (IFNβ) according to the manufacturer's instructions.

AJRCCM Articles in Press. Published on 21-November-2017 as 10.1164/rccm.201707-1475OC

Interferon bioassay. The activity of mouse type I IFN was measured using the reporter cell line B16-Blue IFNα/β (Invivogen) and QUANTI-blue substrate (Invivogen) according to the manufacturer's instructions.

Statistics. Unless otherwise indicated, the statistical differences between groups were determined by non-parametric two-tailed Mann-Whitney test or two-tailed Wilcoxon test or parametric Student *t*-tests using GraphPad Prism5 (see Figure legends).

Supplemental Table E1

Symbol	Description	Raw pValue	Adj pValue	Fold change
Gbp11	guanylate binding protein 11 Gene	9.00457120693179e-05	0.035067443749	9.62
Hspa1a	heat shock protein 1A Gene	6.44996906931854e-05	0.031183633311	7.56
Hspa1b	heat shock protein 1A Gene	1.96662236482532e-05	0.019718545306	7.26
Ubd	ubiquitin D Gene	0.000269140857609537	0.044391979271	7.19
Csf1	colony stimulating factor 1 Gene	0.000118252702962162	0.039685370913	6.72
Tgtp1, Tgtp2	T-cell specific GTPase 1 Gene	0.000149731102328906	0.039685370913	6.70
Ly6c1, Ly6c2	lymphocyte antigen 6 complex, locus C1 Gene, locus C2 Gene	0.000138006680464728	0.039685370913	5.00
Oasl2	2'-5' oligoadenylate synthetase-like 2 Gene	3.16463598001847e-05	0.023353031433	4.49
Zbp1	Z-DNA binding protein 1 Gene	5.29876044513977e-05	0.030399430237	3.80
Irf1	interferon regulatory factor 1 Gene	0.000182189946291551	0.039892226114	3.32
Serpina3g	serine (or cysteine) peptidase inhibitor, clade A, member 3G Gene	7.85462998871599e-06	0.015450057187	3.27
Stat1	signal transducer and activator of transcription 1 Gene	1.24090548748054e-05	0.018984475174	3.16
Iigp1	interferon inducible GTPase 1 Gene	0.000132591318373519	0.039685370913	21.22
Usp18	ubiquitin specific peptidase 18 Gene	0.000163817109057389	0.039685370913	2.89
Ifit3	interferon-induced protein with tetratricopeptide repeats 3 Gene	0.000139992256818056	0.039685370913	2.85
Gvin1	Interferon-induced very large GTPase 1 (Very large-inducible GTPase-1)(VLIG-1) Gene	0.000149672765473399	0.039685370913	2.65
Ifit2	interferon-induced protein with tetratricopeptide repeats 2 Gene	0.000174556834120503	0.039892226114	2.54
Pim2, RP23-401M24.5	proviral integration site 2 Gene	0.000202807453557693	0.039892226114	2.27
Tlr7	toll-like receptor 7 Gene	5.88695568258157e-05	0.031175958766	2.20
Oas1g, Oas1a	2'-5' oligoadenylate synthetase 1G Gene	0.000196676243411168	0.039892226114	2.19
Tap1	transporter 1, ATP-binding cassette, sub-family B (MDR/TAP) Gene	0.000202288778513746	0.039892226114	2.15
Mllt3	myeloid/lymphoid or mixed-lineage leukemia (trithorax homolog, Drosophila); translocated to, 3 Gene	0.000233476615713173	0.042863193623	2.14
Psmb9	proteasome (prosome, macropain) subunit, beta type 9 (large multifunctional peptidase 2) Gene]	4.98784674747506e-06	0.013735532373	2.12
Isg20	interferon-stimulated protein Gene	0.0001204563562551	0.039685370913	2.0
Brwd1	bromodomain and WD repeat domain containing 1 Gene	4.00918155031411e-05	0.025092009439	0.49
Cdc42	cell division cycle 42 homolog (S. cerevisiae) Gene	3.22251141863212e-05	0.023353031433	0.48
Klrd1	killer cell lectin-like receptor, subfamily D, member 1 Gene	0.00017725257793915	0.039892226114	0.39
Gls	glutaminase Gene	3.21793709251226e-06	0.011076943956	0.32
Ncoa3	nuclear receptor coactivator 3 Gene	2.71161074683876e-06	0.011076943956	0.32
Klra9, Klra3	killer cell lectin-like receptor subfamily A, member 9 Gene; member 3 Gene	2.48323386994304e-05	0.021369779472	0.14

AJRCCM Articles in Press. Published on 21-November-2017 as 10.1164/rccm.201707-1475OC

Supplemental Table E2. Murine primers used for real-time PCR

Target	Forward sequence	Reverse sequence
Hprt[1]	5'-GTTCTTTGCTGACCTGCTGGAT-3'	5'-CCCCGTTGACTGATCATTACAG-3'
Stat1	5'-CCATGTCTCCAGAGGAGTTTGAT-3'	5'-GTCGCCAGAGAGAAATTCGTG-3'
Csf1	5'-ACAGGTGGAACTGCCAGTATAGAAAG-3'	5'-GACCCCATCAAAGCTGCTTC-3'
Irgm1	5'-GCGTCACTCGGATCTTATCATG-3'	5'-GAGTAGTGGAGCAGCCTCGC-3'
Tnfsf10	5'-GCTGTGTCTGTGGCTGTGACTTAC-3'	5'-TCATCCGTCTTTGAGAAGCAAGC-3'
Ccl2	5'-CCACTCACCTGCTGCTACTCATTC-3'	5'-TTCCTTCTTGGGGTCAGCACAGAC-3'
Ifnb[2]	5'-GCACTGGGTGGAATGAGACT-3'	5'-AGTGGAGAGCAGTTGAGGACA-3'
Fizz1	5'-TGCCCTGCTGGGATGACT-3'	5'-AGTTGCAAGTATCTCCACTCTGGA-3'
Ym1	5'-TACCCTATGCCTATCAGGGTAATGA-3'	5'-CCTTGAGCCACTGAGCCTTC-3'
Cxcl9	5'-AGCAGTGTGGAGTTCGAGGAAC-3'	5'-AGGGATTTGTAGTGGATCGTGC-3'
Nos2	5'-TCCTCACGCTTGGGTCTTGTTC-3'	5'-TCCAACGTTCTCCGTTCTCTTGC-3'
Mrc1	5'-AATGCCAAAAATTATTGATCCTGTAACT-3'	5'-ACGGTGACCACTCCTGCTG-3'
Ifng	5'-CAGCAACAGCAAGGCGAA-3'	5'-GGACCTGTGGGTTGTTGACCT-3'
Tnf	5'-CAAAATTCGAGTGACAAGCCTGTA-3'	5'-CCACTTGGTGGTTTGCTACGA-3'
Ccrl2	5'-ATCCCTTGAGAGAAAAAATATCAAGC-3'	5'-TCCATCGGAGGCTGTCCTT-3'
Ccl5	5'-CTCCCTCGCGCTGCC-3'	5'-TTCCTTCGAGTGACAAACACGA-3'
Arg1	5'-AATGAAGAGCTGGCTGGTGTGGTG-3'	5'-ATGCTTCCAACTGCCAGACTGTG-3'

1 Benard, A. *et al.* Delta opioid receptors mediate chemotaxis in bone marrow-derived dendritic cells. *Journal of neuroimmunology* **197**, 21-28, doi:10.1016/j.jneuroim.2008.03.020 (2008).

2 Gautier, G. *et al.* A type I interferon autocrine-paracrine loop is involved in Toll-like receptor-induced interleukin-12p70 secretion by dendritic cells. *The Journal of experimental medicine* **201**, 1435-1446, doi:10.1084/jem.20041964 (2005).

Supplemental Table E3. Human primers used for real-time PCR

Target	Forward sequence	Reverse sequence
MLN51[1]	5'-TAATCCCAGTTACCCTTATGCTCCA-3'	5'-GTTATAGTAGGTCACTCCTCCATATACCTGT-3'
CYLD	5'-GCATACGGGTCCTGGCATCTTGTCC-3'	5'-ATGGTGATCTTCTTGCTGGTCTTGC-3'
IFNB[2]	5'-AGCTGCAGCAGTTCCAGAAG-3'	5'-AGTCTCATTCCAGCCAGTGC-3'
CCL2	5'-TGTCCCAAAGAAGCTGTGATCTT-3'	5'-GGTTTGCTTGTCCAGGTGGT-3'

1 Benard, A. *et al.* mu-Opioid receptor is induced by IL-13 within lymph nodes from patients with Sezary syndrome. *The Journal of investigative dermatology* **130**, 1337-1344, doi:10.1038/jid.2009.433 (2010).

2 Gautier, G. *et al.* A type I interferon autocrine-paracrine loop is involved in Toll-like receptor-induced interleukin-12p70 secretion by dendritic cells. *The Journal of experimental medicine* **201**, 1435-1446, doi:10.1084/jem.20041964 (2005).

AJRCCM Articles in Press. Published on 21-November-2017 as 10.1164/rccm.201707-1475OC

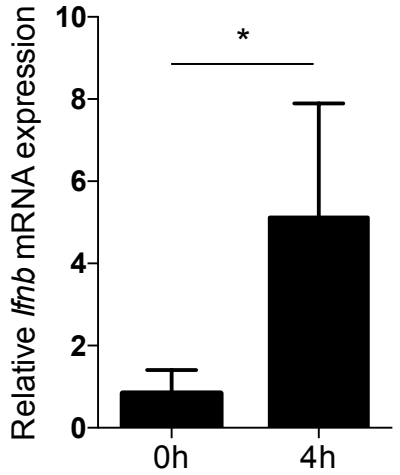

Figure E1. Type I IFN expression by B cells after 4 hours of Mtb stimulation. *Ifnb* mRNA expression in B cells purified from the spleen of WT mice upon stimulation for 4 h with Mtb (MOI=0.5); (n=6). The results were analyzed using a two-sided Mann-Whitney test (* $p<0.05$)

Figure E1

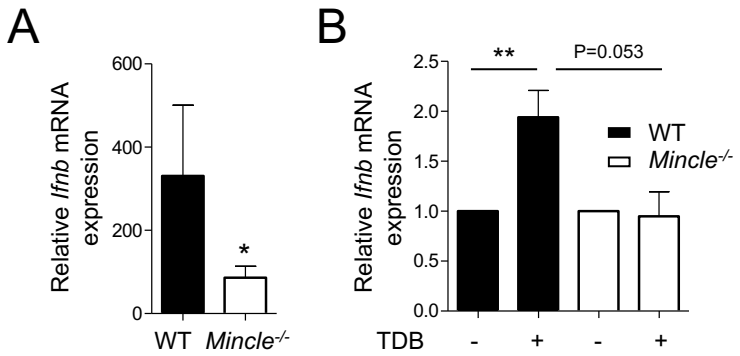

Figure E2. Mincle and its ligand trigger type I IFN expression in B cells. A) *Ifnb* mRNA expression in B cells purified from the spleen of WT (black bars) or *Mincle*$^{-/-}$ (white bars) upon stimulation for 24h with Mtb (MOI=0.3); fold change represent expression after 24h of stimulation relative to respective expression before stimulation (n=5 to 10 mice per group). B**)** *Ifnb* mRNA expression in B cells purified from the spleen of naive WT (black bars) or *Mincle*$^{-/-}$ (white bars) mice stimulated (+) or not (-) with TDB (n=4 per group). Results were analyzed using the two-tailed Mann-Whitney or the two-tailed Wilcoxon test *P≤0.05; ** P≤0.01; *** P≤0.001.

Figure E2

AJRCCM Articles in Press. Published on 21-November-2017 as 10.1164/rccm.201707-1475OC

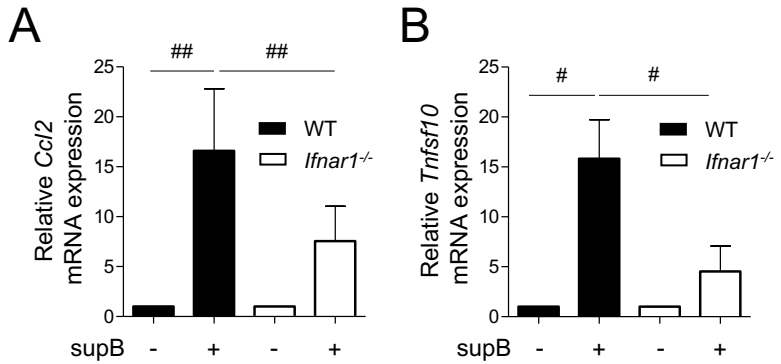

Figure E3. IFNβ production by B cells polarizes macrophages *in vitro* toward an anti-inflammatory phenotype. A, B) Expression of IFN-stimulated genes *Ccl2* (A) and *Tnfsf10* (B) in macrophages prepared from the bone marrow of naive WT or *Ifnar1*$^{-/-}$ mice (n=7 mice per group) upon 4h incubation or not with supernatants from Mtb-stimulated B cells (supB). Results were analyzed using the two-tailed Student's paired *t*-tests. #P≤0.05; ## P≤0.01; ### P≤0.001.

Figure E3

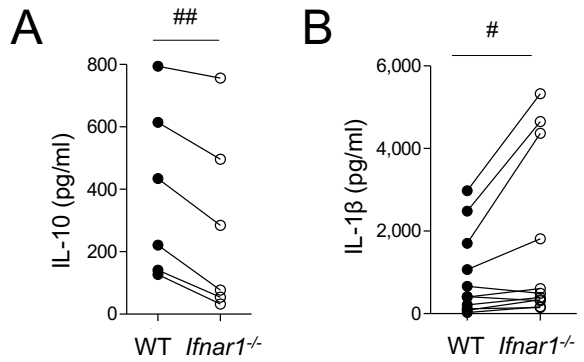

Figure E4. IFNβ production by B cells polarizes macrophages *in vitro* toward an anti-inflammatory phenotype. Concentration of IL-10 (A) and IL-1β (B) in supernatants of WT or *Ifnar1*$^{-/-}$ macrophages first conditioned with supernatant of Mtb-stimulated B cells, and then infected with Mtb (MOI=0.5; n=6 to 8 independent preparations of B cells per group incubated separately with WT or *Ifnar1*$^{-/-}$ macrophages). Results were analyzed using the two-tailed Student's paired *t*-tests (# P≤0.05; ## P≤0.01; ### P≤0.001).

Figure E4

AJRCCM Articles in Press. Published on 21-November-2017 as 10.1164/rccm.201707-1475OC

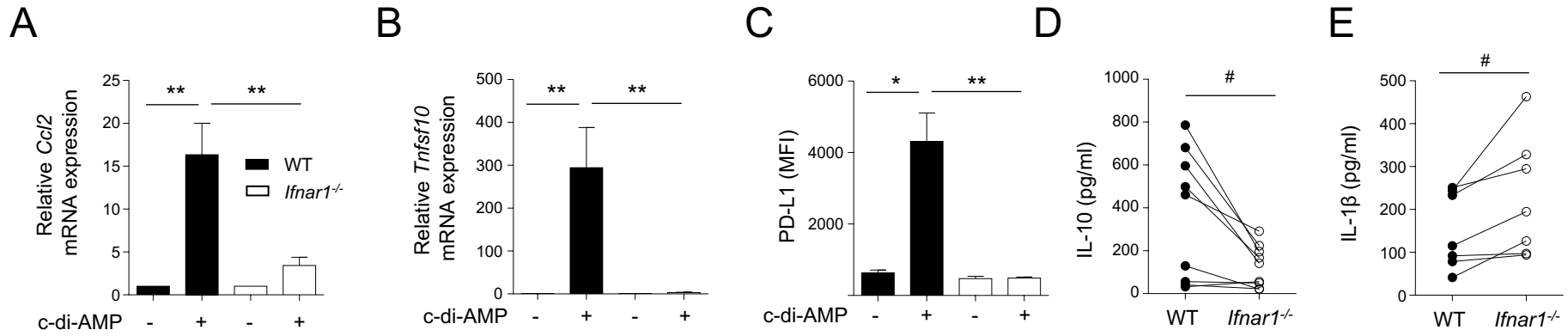

Figure E5. IFNβ production by B cells stimulated with c-di-AMP polarizes macrophages *in vitro* toward an anti-inflammatory phenotype. A, B) Expression of IFN-stimulated genes *Ccl2* (a) and *Tnfsf10* (b) in macrophages prepared from the bone marrow of naive WT or *Ifnar1*$^{-/-}$ mice (n=7 mice per group) upon 4h incubation or not with supernatants from c-di-AMP-stimulated B cells. C) mean fluorescence intensity (MFI) of PD-L1 surface expression on macrophages derived from the bone marrow of naive WT or *Ifnar1*$^{-/-}$ mice and incubated (+) or not (-) for 24h with supernatants of c-di-AMP-stimulated B cells (n=4 independent preparations of B cells per group). D, E) Concentration of IL-10 (D) and IL-1β (E) in supernatants of WT or *Ifnar1*$^{-/-}$ macrophages first conditioned with supernatant of c-di-AMP-stimulated B cells, and then infected with Mtb (MOI=0.5; n=6 to 8 independent preparations of B cells per group incubated separately with WT or *Ifnar1*$^{-/-}$ macrophages). Data represent mean±s.e.m., and are representative of the indicated number of independent experiments. Results were analyzed using the two-tailed Mann-Whitney test or the Wilcoxon test *P≤0.05; ** P≤0.01; *** P≤0.001 (A-C) and the two-tailed Student's paired *t*-tests (D,E). #P≤0.05; ## P≤0.01; ### P≤0.001.

Figure E5

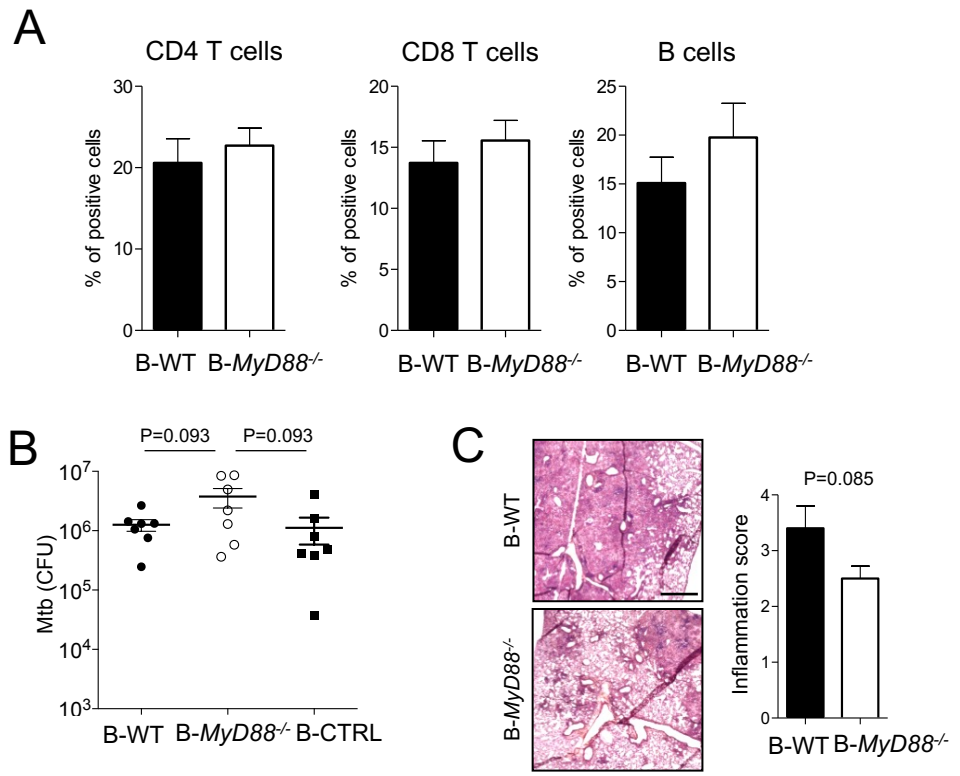

Figure E6. MyD88 deficiency in B cells results in reduced lung inflammation and bacterial control in Mtb-infected mice. Mixed bone marrow chimeras were generated in which B cells were competent (B-WT, i.e. 80% mMT + 20%WT→ WT, black bars or symbols) or deficient (B-*MyD88*$^{-/-}$, i.e. 80% mMT + 20% *MyD88*$^{-/-}$→WT, white bars or symbols) for *MyD88*. B-CTRL mice (80% WT + 20% *MyD88*$^{-/-}$→WT) lacking *MyD88* expression on 20% total hematopoietic cells were also used as control. These mice were infected with 1000 CFUs Mtb, H37Rv strain, and their lungs analyzed 6 weeks later. A) Percentages of CD4^{+} T (left), CD8^{+} T (middle) and CD19^{+} B (right) cells in the lung of B-WT and B-*MyD88*$^{-/-}$ mice (n=7). B) Bacterial loads (colony forming units, CFUs) in the lungs of B-WT, B-*MyD88*$^{-/-}$, and B-CTRL mice (n=7). C) Representative hematoxylin and eosin staining in lung sections from B-WT and B-*MyD88*$^{-/-}$ mice (left panels), and blind scoring of inflammation (right panels) (n=3 mice per group). Bar represents 1 mm (n=3). Data represent mean±s.e.m., are representative of two independent experiments, and were analyzed using the two-tailed unpaired Student's *t*-tests.

Figure E6